



HAL
open science

**Rare Earth Element sorption by basaltic rock:
experimental data and modeling results using the
“Generalised Composite approach”.**

E. Tertre, A. Hofmann, G. Berger

► **To cite this version:**

E. Tertre, A. Hofmann, G. Berger. Rare Earth Element sorption by basaltic rock: experimental data and modeling results using the “Generalised Composite approach”. *Geochimica et Cosmochimica Acta*, 2007, 72, pp.1043-1056. 10.1016/j.gca.2007.12.015 . hal-00450682

HAL Id: hal-00450682

<https://hal.science/hal-00450682>

Submitted on 26 Jan 2010

HAL is a multi-disciplinary open access archive for the deposit and dissemination of scientific research documents, whether they are published or not. The documents may come from teaching and research institutions in France or abroad, or from public or private research centers.

L'archive ouverte pluridisciplinaire **HAL**, est destinée au dépôt et à la diffusion de documents scientifiques de niveau recherche, publiés ou non, émanant des établissements d'enseignement et de recherche français ou étrangers, des laboratoires publics ou privés.

Rare Earth Element sorption by basaltic rock: experimental data and modeling results using the “Generalised Composite approach”.

Tertre E.^{1*}, Hofmann A.¹ and Berger G.²

¹ Université des Sciences et Technologies de Lille1, UMR PBDS 8110, 59655 Villeneuve d’Ascq, France.

² Université Toulouse III, UMR LMTG 5563, 14 av. E. Belin, 31400 Toulouse, France.

*Author to whom correspondence should be addressed:

Emmanuel TERTRE
Hydrasa – Bat. Sciences Naturelles
40 Avenue du recteur Pineau
86000 Poitiers – France

Email address : emmanuel.tertre@univ-poitiers.fr

Keywords: sorption, lanthanides, basalt, surface complexation, « Generalised Composite model », exchange sites, specific sites.

Abstract

Sorption of the 14 Rare Earth Elements (REE) by basaltic rock is investigated as a function of pH, ionic strength and aqueous REE concentrations. The rock sample, originating from a terrestrial basalt flow (Rio Grande do Sul State, Brazil), is composed of plagioclase, pyroxene and cryptocrystalline phases. Small amounts of clay minerals are present, due to rock weathering. Batch sorption experiments are carried out under controlled temperature conditions of 20°C with the < 125 µm fraction of the ground rock in solutions of 0.025 M and 0.5 M NaCl and at pH ranging from 2.7 to 8. All 14 REEs are investigated simultaneously with initial concentrations varying from 10⁻⁷ to 10⁻⁴ mol/L. Some experiments are repeated with only europium present to evaluate possible competitive effects between REE. Experimental results show the preferential retention of the heavy REEs at high ionic strength and circumneutral pH conditions. Moreover, results show that REE sorption increases strongly with decreasing ionic strength, indicating two types of sorption sites: exchange and specific sites. Sorption data are described by a Generalised Composite (GC) non-electrostatic model: two kinds of surface reactions are treated, i.e. cation exchange at >XNa sites, and surface complexation at >SOH sites. Total site density (>XNa + >SOH) is determined by measuring the cation exchange capacity (CEC = 52 µmol/m²). Specific concentrations of exchange sites and complexation sites are determined by fitting the Langmuir equation to sorption isotherms of REE and phosphate ions. Site densities of 22 ± 5 and 30 ± 5 µmol/m² are obtained for [>XNa] and [>SOH], respectively. The entire set of REE experimental data is modelled using a single exchange constant (log K_{ex} = 9.7) and a surface complexation constant that progressively increases from logK = -1.15 for La(III) to -0.4 for Lu(III).

The model proves to be fairly robust in describing other aluminosilicate systems. Maintaining the same set of sorption constants and only adjusting the site densities, we obtain good agreement with literature data on REE/kaolinite and REE/smectite sorption. The Generalised Composite non-electrostatic model appears as an easy and efficient tool for describing sorption by complex aluminosilicate mineral assemblages.

INTRODUCTION

Over the past four decades, numerous studies have been carried out on rare earth element (REE) behavior during geological and geochemical processes, in view of their role as markers of geological sources and also because they are analogues of transuranic radioelements. Fractionation of REE abundance patterns is often recorded in magmatic rocks and precipitates of hydrothermal fluids (Masuda and Akagi, 1989; Kawabe *et al.*, 1991; Akagi *et al.*, 1993; Lee *et al.*, 1994; Sholkovitz *et al.*, 1994; Kawabe, 1995; Bau *et al.*, 1996; Irber, 1999; Monecke *et al.*, 2002; Takahashi *et al.*, 2002). The tetrad effect is reflected by a specific REE pattern observed in certain solid phases, resulting from increased stability at quarter, half, three-quarter and complete filling of the 4f electron shell, and has been particularly highlighted and interpreted by Masuda and Akagi (1989), Kawabe *et al.* (1991), Lee *et al.* (1994), Kawabe (1995), Bau *et al.* (1996), and Irber (1999). Nevertheless, as mentioned by McLennan (1994) and Monecke *et al.* (2003), certain tetrad effects reported in the literature are only apparent and some observations (Kawabe *et al.*, 1991; Akagi *et al.*, 1993; Takahashi *et al.*, 2002) should be considered with caution given the uncertainties of the analytical methods used.

Another aspect concerning REE geochemistry is the sorption of these elements onto mineral surfaces. Many experimental studies have been carried out to quantify the retention of these elements on mineral surfaces using multiple REE patterns. Some of these studies consider synthetic minerals and solutions (Kagi *et al.*, 1993; De Carlo *et al.*, 1998; Bau, 1999; Kawabe *et al.*, 1999; Ohta and Kawabe, 2001; Davranche *et al.*, 2004 and 2005; Quinn *et al.*, 2004, 2006a and b), while others deal with synthetic minerals and natural waters (Byrne and Kim, 1990; Koeppenkastrop and De Carlo, 1992; De Carlo *et al.*, 1998) or natural minerals and synthetic solutions (Byrne and Kim, 1990; Coppin *et al.*, 2002; Tao *et al.*, 2004; Tang and Johannesson, 2005; Tertre *et al.*, 2005). Otherwise, Balistrieri *et al.* (1981) have investigated natural solids in contact with natural waters. Koeppenkastrop and De Carlo (1992) have studied the sorption of the 14 REE from seawater by synthetic mineral particles (hydroxyapatite, goethite and vernadite), showing that LREE (Light REE) are more strongly retained than HREE (Heavy REE) during the sorption process. This behavior was explained by these authors, as well as by Quinn *et al.* (2006b), by taking into account the fractionation of aqueous complexes. On the other hand, Coppin *et al.* (2002) and Tertre *et al.* (2005) showed that, for neutral pH and in high ionic strength solutions, LREE sorbed less readily on clay mineral surfaces (kaolinite and montmorillonite) than HREE. This particular behavior is compatible with results on REE sorption by amorphous ferric hydroxide (Bau, 1999; Ohta and

Kawabe, 2001; Quinn *et al.*, 2006a and b) or natural sand (Tang and Johannesson, 2005). The sorption of a given REE on different minerals surfaces (iron oxides, aluminum oxides, clay minerals, etc.) has been intensively investigated in the framework of strategies for radioactive waste disposal. In these studies, the main objective was to understand the fundamental processes of sorption and perform quantitative modeling of sorption by advanced surface complexation models. Bradbury and Baeyens (2002) and Tertre *et al.* (2006b) studied sorption of europium onto montmorillonite and kaolinite, whereas Sinitsyn *et al.* (2000) and Kulik *et al.* (2000) investigated sorption of neodymium and europium onto an illite. Marmier and Fromage (1999), Rabung *et al.* (2000) and Kowal-Fouchard (2002) worked on Eu sorption by using aluminum oxides. Surface investigations most often focus on europium data only. However, Quinn *et al.* (2006a and b) proposed a surface complexation model for sorption of the 14 REE by amorphous ferric hydroxide. Generally, due to the number of mutually dependent parameters, surface complexation models include many parameters that must be constrained by physical measurements and thus do not rely solely on fitting. The following parameters can be constrained: (1) the site density values, (2) the surface potential of the mineral, and (3) the stoichiometry of the sorbed species. Site density values can be constrained by crystallographic data, interpretation of acid/base titrations or cationic exchange capacity (CEC), while the surface potential of minerals can be estimated from electrokinetic measurements (i.e. zeta potential). In some cases, the stoichiometry of the surface species is approached by spectroscopic investigations, such as TRLFS (Stumpf *et al.*, 2001; Kowal-Fouchard *et al.*, 2004; Rabung *et al.*, 2005) or EXAFS (Stumpf *et al.*, 2004).

Despite the considerable knowledge acquired about REE retention at the atomic scale, the prediction of REE sorption at the whole-rock scale is still a challenge because of the mineralogical complexity of natural rocks (nature of the phase in contact with water, nature and density of sites, surface area). Different approaches have been used to model whole-rock or bulk sediment sorption processes. El Aamrani *et al.* (2002), Barnett *et al.* (2002), Davis *et al.* (2004) and Payne *et al.* (2004) interpreted sorption data of Uranium VI by olivine rock, different American soils, an aquifer sediment and a weathered shale, using either (1) the component additivity model (CA) or (2) the Generalised Composite model (GC). These two approaches were described in detail by Davis *et al.* (1998) and Davis *et al.* (2004). Briefly, the CA approach assumes that the sorption properties of a mineral assemblage (sediment, rock, soil, etc.) are the sum of the sorption properties of the individual phases making up this assemblage. Therefore, by knowing the properties of the major phases of the assemblage, we can calculate the properties of the mineral assemblage without further adjustment using experimental data obtained from the mixture. On the contrary, the GC approach assumes that a

mineral assemblage is too complex to be described as a superposition of the individual phases. In this approach, sorption is described using generic sites (called >SOH) and the values of the site densities and formation constants are obtained by fitting the experimental data.

Application of the CA model to the retention of REE by silicate rocks is difficult because of the lack of sorption data on common minerals such as feldspars, pyroxenes, etc. On the other hand, the GC approach requires whole-rock sorption data, which, to our knowledge, are not available in the literature for basaltic rock.

In the present article, we study sorption of the 14 REE by a basaltic rock and develop a simple surface complexation model able to interpret experimental data dependent on pH and ionic strength. No such model has so far been developed for a basaltic material. Although basalt is a widespread rock on the Earth's surface, and despite its use in various industrial applications, it has been neglected in sorption studies. By analogy with mechanistic studies on clay minerals (Kulik *et al.*, 2000; Bradbury and Baeyens, 2002; Tertre *et al.*, 2006b), we consider *a priori* two kinds of fundamental processes: exchange with pre-existing cations linked to the surface by electrostatic bonds (outer-sphere type complexes) and specific surface complexation (inner-sphere type complexes) with hydrolysed sites such as silanol, ferrinol and aluminol. Then, by considering two generic sites (an exchange and a complexation site), we show it is possible to describe the REE sorption on basalt within the framework of a non-electrostatic GC model.

MATERIALS AND EXPERIMENTAL METHODS

Basalt sample:

The raw material is a natural basaltic rock collected from a subaerial volcanic flow in the Alta Uruguay region in the northern part of the Rio Grande do Sul State, Brazil. This 15-35 m thick volcanic flow was erupted during the Jurassic-Cretaceous transition. The rock formation has been well preserved from weathering. Detailed geological, petrological, and geochemical descriptions have been reported by Gomes (1996), Scopel (1997), Schenato *et al.* (2003) and Fischer (2004). Briefly, the selected samples were extracted from the massive core (least altered part) of the lava flow and are made up of a cryptocrystalline groundmass with phenocrysts of plagioclase (An₄₂ to An₇₀), pyroxene (augite and pigeonite) and minor K-feldspar, quartz and acicular Ti-magnetite. The groundmass is composed of K-feldspar, albite, clays (chlorite/saponite), quartz and apatite. These phases are clearly identified in SEM/backscattered images and SEM/EDS analyses (Schenato *et al.*,

2003). The chemical composition and REE contents of the basalt, reported in Table 1, are taken from Fischer (2004).

In our study, we crushed the natural samples and selected the 0-125 μm size fraction as material for the experiments. To preserve a high specific surface area, we did not separate the grains from the fine particles generated by crushing. The potentially existing exchangeable sites were saturated with Na^+ by treating the crushed material with 0.025 M NaCl solution. This procedure was repeated three times, and after each dispersion, the suspension was centrifuged, the supernatant removed and replaced by a new solution. Finally, the conditioned basalt powder was dried at 40°C and stored in closed containers. The mineralogical composition of the conditioned powder was determined by X-Ray diffraction (XRD), which detected the presence of anorthite, augite and pigeonite. Trace amounts of K-feldspar were also observed. Oriented and glycolated samples, prepared from the finest size fraction (0-0.45 μm), indicated the presence of smectites (reflection at 17Å). Semi-quantitatively, the clay fraction was estimated to account for less than 2 % of the material.

The surface area of the 0-125 μm size fraction, determined by N_2 -gas adsorption (BET), was found to be 1.8 $\text{m}^2\cdot\text{g}^{-1}$. This surface area is much higher than the values generally found for cleaned size fractions (few hundreds of $\text{cm}^2\cdot\text{g}^{-1}$), probably due to the small quantities of smectite, since smectites have a high specific surface area ($S_{\text{BET}} \approx 30$ to 800 $\text{m}^2\cdot\text{g}^{-1}$; see discussions in Tournassat *et al.* (2003) and Tertre *et al.*, 2006a). The cation exchange capacity (CEC) was measured at the Laboratoire Environnement et Minéralurgie at Nancy, France, with the copper-tetramine method (Meier and Kahr 1999), performed in deionized water at pH =7. The CEC was found to be 9.4 ± 0.3 meq/100g (i.e. 52 $\mu\text{mol}/\text{m}^2$).

Sorption experiments

Sorption envelopes of the 14 REE at given initial aqueous concentrations were examined as a function of pH and ionic strength. To investigate possible sorption competition between the 14 REE, some additional envelopes were determined with “Eu only”. Sorption isotherms were also measured. Generally isotherms were determined at given pH and ionic strengths with “Eu only”. Again, to identify possible competitive effects, some additional isotherms were obtained with all the 14 REE present.

All the experiments were carried out at $20 \pm 1^\circ\text{C}$ under atmospheric conditions, in closed PTFE containers. Samples had a constant solid/solution ratio of 2.5 g.L^{-1} ; the background concentration was 0.025 M or 0.5 M NaCl (Prolabo, RP Normapur). For some solutions, total aqueous carbonate concentrations were measured by acid/base titration to quantify the saturation state of the solutions with respect to atmospheric CO_2 ($p_{\text{CO}_2}=10^{-3.5}$). Solutions with circumneutral pH (6 to 8) and $I=0.025 \text{ M}$ had total aqueous carbonate concentrations less than or equal to around $1.5 \times 10^{-5} \text{ mol/L}$, indicating that our solutions were CO_2 -undersaturated at $\text{pH}=8$ or practically saturated at $\text{pH}=6$. The sorption envelopes were measured between pH 2.7 and 8, and sorption isotherms were determined with pH buffered at 5.6 ± 0.2 . The pHs were stabilised using small quantities of HClO_4 (Prolabo, RP Normapur) and NaOH (Prolabo, RP Normapur). We preferred using HClO_4 rather than HCl, so as to obtain the same concentration of chloride in all experiments. The stock solution containing the 14 REE, each at a concentration of 10 ppm, was prepared from a standard solution of 100 ppm in 2% HNO_3 (Spectrascan TEKNOLAB A/S). The pH of the 14 REE stock solution was increased to $\text{pH}=2$ by adding small quantities of NaOH to prevent a significant decrease in pH of the basalt suspension after the addition of REE. Europium stock solution was prepared using a similar procedure.

For the sorption envelope experiments, the initial REE concentration was fixed at 100 ppb for each REE (i.e. 5.7×10^{-7} to $7.1 \times 10^{-7} \text{ mol/L}$ depending on the lanthanide). For Eu-isotherms and for “all REE” isotherms, total concentration of each REE varied between 6.5×10^{-7} and $1.3 \times 10^{-4} \text{ mol/L}$. Before REE addition, the suspension was equilibrated for one week at the desired pH and ionic strength. After REE addition, equilibrium was considered to be reached after three days based on previous work on REE-clay systems (Lauber *et al.*, 2000, and Coppin *et al.*, 2002). Finally, the solution was extracted by centrifugation at 3000g for 15 minutes. The efficiency of solid/solution separation under these centrifugation conditions was checked by measuring the concentrations of aluminum and silica in the supernatant (ICP-MS, Perkin-Elmer Elan-6000). The maximum aqueous silica concentration was found to be always below 10 ppm, while aqueous aluminum was less than

0.2 ppm. The aqueous Si value and the Al/Si ratios can be readily explained by the incongruent dissolution of the basaltic sample. The low Al/Si ratio in solution does not fit with any of the basalt-forming components. This makes it unlikely that the supernatant contains any basaltic colloids. As we could not avoid slight basalt dissolution during the experiments, all basalt suspensions were pre-equilibrated before REE addition as mentioned above. The supernatant was divided into two aliquots, the first was used for pH measurement, whereas the second was acidified with HNO₃ 2% prior to REE analysis. Whatever the ionic strength, the pH was measured at 20°C with a Mettler Toledo[®] combined electrode. At I=0.025 M, the electrode was calibrated on an activity scale with three buffer solutions (pH=4.01, pH=7.00 and pH=9.21). When the electrodes are transferred from the calibration solution to the measurement solution, a small residual liquid junction potential can still develop so the hydrogen-ion activity read on the pH-meter may deviate very slightly from the absolute value. At I=0.5 M the liquid junction potential is much higher than at I=0.025 M. Therefore, the electrode was calibrated on a concentration scale using HCl/NaCl or NaOH/NaCl solutions at the same ionic strength. In this case, the H⁺ activity coefficient needed to calculate the corresponding pH was computed using the Davies equation ($\gamma_{\text{H}^+} = 0.436$). The Davies equation is not an ideal choice for high ionic strength conditions. Nevertheless, because we had to use a single activity law during the sorption study to obtain consistent calculations with the CHESS[®] code, we chose the Davies formalism as the best “compromise” for conditions of widely varying ionic strength. The pH uncertainty of ± 0.2 given for the sorption isotherms does not correspond to the uncertainty of an individual measurement, which is smaller than 0.05 pH units, but rather to the mean pH difference of all individual samples of one isotherm experiment. Indeed, we preferred adjusting the pH of each sample only with strong acid or base rather than a pH buffer, in order to avoid REE complexation with organic ligands of the buffer solution.

The aqueous REE concentrations were analysed by ICP-MS. The detection limit is 20 ppt for each of the REE and the analytical precision is around 5%. Instrumental instabilities were corrected using ¹¹⁵In and ¹⁸⁷Re as internal standards.

To distinguish between exchange and specific sites at the basalt surface, a few additional sorption isotherms were performed with an anion (phosphate). As with the REE, phosphate sorption isotherms were determined at two different ionic strengths (0.025 and 0.5 M NaCl), total phosphate concentrations ranging from 10⁻⁴ to 8x10⁻³ mol/L, at a pH of 4.7±0.2. For oxide minerals, this pH corresponds to conditions of optimal adsorption (Barrow *et al.*, 1980). The stock solution of phosphate was prepared from KH₂PO₄ salt (Prolabo, RP Normapur). Dissolved phosphate present in the supernatant at the end of the reaction was analysed using the phosphomolybdate blue

colorimetric method (APHA *et al.*, 1998). The dominant P species in solution is H_2PO_4^- , which is amphoteric because it forms part of two acid/base couples: $\text{H}_3\text{PO}_4/\text{H}_2\text{PO}_4^-$ ($\text{pK}_{\text{a}1}=2.12$) and $\text{H}_2\text{PO}_4^-/\text{HPO}_4^{2-}$ ($\text{pK}_{\text{a}2}=7.2$). These couples buffer the solution at a pH close to 4.7. In the case of Eu, the experimental constraints lead us to use a pH of 5.6 ± 0.2 , which is not the pH of maximal adsorption. Nevertheless, because of the very large concentration interval for the Eu isotherm, it is likely that saturation of >SOH sites was attained in our experiments.

Possible artifacts in sorption experiments

The amounts of REE adsorbed by the basalt sample are calculated from the difference between total and equilibrium concentrations. The calculations require that no other reactions interfere, such as adsorption by the PTFE containers, release of REE by the sample itself or precipitation of solid phases incorporating REE. Adsorption on the container walls has been tested in a previous study with clays (Tertre *et al.*, 2005); it is negligible under acidic conditions and represents only a few percent of the starting concentration under neutral and alkaline conditions (less than 6% when $\text{pH}<8$). The possible release of REE by the basalt sample itself was estimated in a batch experiment in 0.5 M NaCl at pH 4 without addition of REE. After one week of reaction, the aqueous concentrations were less than 40 ppt, which is negligible when compared to the 100 ppb introduced for the sorption experiments. The third possible artifact, precipitation of solid phases, was tested by thermodynamic calculations. The chemical stability and detailed speciation of the experimental solutions before sorption were calculated using the code PHREEQC[®] (Parkhurst, 1995) and the data base reported in appendix A. For the 14 REE, thermodynamic constants are those proposed by Luo and Byrne (2004) for REECO_3^+ and $\text{REE}(\text{CO}_3)_2^-$, and those of Klungness and Byrne (2000) for REEOH^+ . Since our calculations involve solutions having pH 2-8, we do not take into account other hydrolysis species (i.e. $\text{REE}(\text{OH})_2^+$, $\text{REE}(\text{OH})_{3\text{aq}}$ and $\text{REE}(\text{OH})_4^-$). The database also contains solubility constants for solids which could eventually precipitate, such as $\text{REE}(\text{OH})_{3(\text{s})}$, REEOHCO_3 and $\text{REE}_2(\text{CO}_3)_{3(\text{s})}$. For these solids, we use the constants proposed by Johnson *et al.* (1992). Calculations are performed for 0.5 M NaCl solutions, with pH varying from 2 to 8, containing 100 ppb of each aqueous REE and assuming equilibrium with atmospheric CO_2 . The assumption of equilibrium with atmospheric pCO_2 ($\text{pCO}_2=10^{-3.5}$) is a strong constraint since, above pH 6, the sample solutions tend to be undersaturated with regard to CO_2 concentrations. For pH lower than 7, the

starting solutions are undersaturated with respect to possible hydroxides and carbonate phases, and free REE^{3+} is the main species of REE in solution. When $\text{pH} = 7-8$, REECO_3^+ becomes the dominant aqueous species, and some solids such as $\text{NdOHCO}_{3(s)}$, $\text{La}_2(\text{CO}_3)_3(\text{H}_2\text{O})_{8(s)}$ and $\text{Ce}_2(\text{CO}_3)_3(\text{H}_2\text{O})_{8(s)}$ can precipitate from the starting solution. However, this range of pH also corresponds to high sorption. In the experiments, the final aqueous concentrations of REE under these pH conditions are significantly below the solubilities of these solids and appear to be controlled by equilibrium with the sorbed species. An additional argument against precipitation under the experimental conditions is that a similar uptake is observed for all of the 14 REE. With precipitation, REE removal from solution would have led to a stepped pattern from lower to higher pH for elements with increasing atomic number from LREE to HREE. For the Eu isotherm experiments in particular ($\text{pH}=5.6$ and $C_{\text{Eu}} = 6.5 \times 10^{-7}$ to 1.3×10^{-4} mol/L), calculations show that Eu^{3+} is always the major aqueous species of Eu(III), whereas $\text{Eu}(\text{OH})_{3(s)}$ and carbonate phases do not precipitate. For phosphate isotherm measurements, speciation calculations performed with the SUPCRT 92 data base (Johnson *et al.*, 1992) predict that H_2PO_4^- is the main aqueous phosphate species between pH 3 and 7, and that the solutions never approach saturation with respect to any phosphate phase, even at the higher initial concentration (i.e. 8×10^{-3} mol/L).

Modeling method

Modeling calculations are performed with the CHES[®] computer code and the database reported in Appendix A. Aqueous activity coefficients are calculated using the Davies approximation. Sorption is described by the non-electrostatic interface model (NEM). The surface sites are described in the framework of the Generalised Composite approach of Davis *et al.* (1998 and 2004). The concept is presented in more detail below in the “surface complexation modeling” section.

RESULTS AND DISCUSSION

Fractionation between REE:

Figures 1A and 1B show the sorption of the 14 REE as a function of the atomic number, at different pH, and for experiments carried out at $I=0.025$ M and $I=0.5$ M, respectively. At both ionic strengths, REE sorption increases strongly with increasing pH, approaching 100% above pH 6.86 at $I=0.025$ M. At low ionic strength ($I=0.025$ M), sorption remains significant under acidic conditions (e.g. 38% at pH 3.7) and all 14 REE show identical behavior. By contrast, we observe preferred sorption of the HREE in the near-neutral region at high ionic strength (i.e. $I=0.5$ M), with a clearly marked tetrad effect. The Lu/La ratio is close to 1.6 at pH=6.5. This fractionation of the REE pattern with a tetrad effect was reported previously in sorption experimental studies performed with clay minerals (Bonnot-Courtois and Jaffrezic-Renault, 1982; Coppin *et al.*, 2002; Tertre *et al.*, 2005), natural sand (Tang and Johannesson, 2005), iron oxyhydroxides (Quinn *et al.*, 2006a) or during precipitation of iron oxyhydroxides (Bau, 1999). Other studies report an opposite fractionation (LREE more strongly sorbed than HREE) during precipitation or sorption with Mn-oxide, hydroxyapatite, goethite and calcium sulphate (Koeppenkastrop and De Carlo, 1992; Kagi *et al.*, 1993). In these latter studies, the fractionation is explained by aqueous complexation of REE with ligands present in seawater, in particular with carbonates (see also Quinn *et al.*, 2006a and b). In sorption studies on clays, REE fractionation is observed only at high ionic strength and neutral pH, as shown in the present experiments. To explain this particular effect, steric constraints can be considered that would make it more difficult to sorb REEs with large ionic radii, i.e. the LREE (Shannon, 1976). Another factor that has been invoked is the decrease of dehydration energy with atomic number (Muecke and Möller, 1988). This last explanation assumes that REEs are sorbed as inner-sphere complexes, which is typically the case with experiments performed in high ionic strength solutions and at neutral pH (Stumpf *et al.*, 2002). We conclude that the tetrad effect observed in our experiments may reflect the formation of inner-sphere complexes at the basalt surface. Similarly, inner-sphere complexation has been inferred from the differences in chemical bonding between pairs of REE(III) ions by Kawabe (1992). On the other hand, at low ionic strength, the smaller influence of pH and the absence of fractionation of the REE abundance pattern suggest that a non-selective and pH-independent mechanism dominates the sorption process, such as exchange with the labile cations of the Na-saturated basalt.

Europium data:

Figure 2 shows the sorption of europium at two ionic strengths, either as a function of pH (Figure 2A), or as a function of aqueous europium at equilibrium (Figure 2B). The adsorption envelopes in Fig. 2A are obtained for europium in the presence (solid symbols) and absence (open symbols) of the other REE. We observe in Fig 2A that europium sorption increases with pH in all cases. At low pH, however, a drastic increase in sorption occurs with decreasing ionic strength. Similarly, the isotherms in Fig. 2B clearly reflect the ionic strength effect. For instance, for an aqueous equilibrium concentration of 10^{-5} mol/L, the quantity of sorbed europium decreases from 5×10^{-6} mol/g at $I=0.025$ M, $\text{pH } 5.6 \pm 0.2$, to 10^{-6} mol/g at $I=0.5$ M.

Sorption of trivalent cations by simple oxides is usually considered as being due to surface complexation, involving formation of inner-sphere complexes with specific ($>\text{SOH}$) sites having acid/base properties (Fe-oxyhydroxide: Marmier *et al.*, 1997; Catalette *et al.*, 1998; Naveau *et al.*, 2005; Quinn *et al.*, 2006a and b. Silica: Marmier, 1994; Komulski, 1997. Alumina: Huang and Stumm, 1973; Marmier, 1994; Rabung *et al.*, 2000; Quinn *et al.*, 2004). The solution ionic strength has only a weak influence on the formation of these complexes (Hayes and Leckie, 1987; Lützenkirchen, 1997; Quinn *et al.*, 2004). By contrast, sorption by clay minerals shows two effects: (1) a pH dependence consistent with the inner-sphere complexation concept, and (2) an ionic strength dependence attributed to outer-sphere complexation at the exchange sites ($>\text{X}^-$, or $>\text{XNa}$ when saturated by Na^+) of the basal surfaces (Bradbury and Baeyens, 2002; Tertre *et al.*, 2006b). The resemblance between the sorption patterns of clay minerals and the basalt suggests that the basalt surfaces have both exchange sites and specific sites. Because sorption at exchange sites is not specific, it is influenced by the presence of other competing cations. One consequence is the ionic strength effect, but competition between the 14 REE may also influence the extent of sorption. According to Fig. 2A, however, there is no difference in the europium sorption data according to whether or not the full REE series is present, suggesting that competition is negligible at the experimental concentrations of 100 ppb for each REE.

SURFACE COMPLEXATION MODELING

Estimation of site densities:

A key parameter in a surface complexation model is the density of reactive sorption sites at the mineral surface. Because this parameter has a physical meaning, it should not be determined solely by model fitting. For example Payne *et al.* (2004) report that, by varying site densities from 0.2 to 20 $\mu\text{mol}\cdot\text{m}^{-2}$, they obtained 12 different surface complexation models to describe sorption data of U(VI) by shales. To propose a realistic set of parameters, we attempt in this study to determine the best possible values for site densities by combining different experimental methods.

The CEC measurements were performed at pH=7 in deionized water, a condition where the main >SOH sites present on the basalt surface are neutral or deprotonated (see pKa of >SiOH and >AlOH). Since the CEC was determined using a copper-tetramine cation and with a solution only containing H^+ as other cations, the measured CEC (9.4 ± 0.3 meq/100g) should reflect the densities of the exchange and the >SOH sites, which are thus representative of the total reaction sites.

The REE sorption experiments were performed with material initially saturated with Na^+ . In addition, all experiments were carried out in the presence of a NaCl electrolyte. We thus can assume that all exchange sites were in the >XNa form prior to REE addition, except at very low pH where Na^+/H^+ exchange occurs (see discussion on modeling further below). However, in the pH range of the exchange measurements (i.e. neutral pH), CEC can be defined as $[\text{>SOH}]_{\text{TOT}} + [\text{>XNa}]_{\text{TOT}}$. To distinguish between >SOH and >XNa sites, we performed specific sorption experiments with both cations and anions (europium and phosphate) under low and high ionic strength conditions. The results are reported in Figures 3A and 3B. The sorption of Eu is dependent on ionic strength, likely because both surface complexation onto >SOH sites occurs along with exchange reactions on >XNa sites. In figure 2A, it can be clearly seen that at any given pH Eu is sorbed more strongly at $I=0.025$ M than at $I=0.5$ M. This implies a greater contribution of exchange reactions at low ionic strength. As a first estimate, we consider that, at $I=0.5$ M, all exchange sites are saturated with Na^+ , whatever the pH, and that Eu is sorbed only onto >SOH sites. Under this hypothesis, the Eu-isotherm performed at $I=0.5$ M can be modeled with a one-site Langmuir reaction curve:

$$[\text{Eu}]_{\text{sorbed}} = S_{\text{max}} \cdot \frac{K_L \cdot [\text{Eu}]_{\text{aq.}}}{1 + K_L \cdot [\text{Eu}]_{\text{aq.}}} \quad (1)$$

where $[Eu]_{sorbed}$ is the concentration of europium sorbed onto the solid (mol/g) and $[Eu]_{aq.}$ is the aqueous Eu concentration at equilibrium (mol/L); $S_{max.}$ and K_L are the fitted site density (mol/g) and the Langmuir constant (L/mol), respectively. The parameters are fitted by matching the Langmuir equation to the experimental data, using a least squares analysis method. We thus obtain a fitted site density of $36 \pm 5 \text{ mol/m}^2 >\text{SOH}$ (i.e. $6.9 \pm 0.9 \times 10^{-5} \text{ mol/g}$) (see Table 2 for the value of $S_{max.}$). To interpret the Eu isotherm carried out at $I=0.025 \text{ M}$, we again use the one-site Langmuir formalism. In this case, we obtain a site density of $50 \pm 6 \text{ } \mu\text{mol/m}^2$ (i.e. $9.0 \pm 1.1 \times 10^{-5} \text{ mol/g}$), a value much higher than that obtained at high ionic strength. The difference between the two site density values ($14.0 \pm 7.8 \text{ } \mu\text{mol/m}^2$) is attributed to the $>\text{XNa}$ site density. This assumption is supported by the slight increase of the Langmuir constant with decreasing ionic strength ($K_L = 2.10^3$ at $I=0.5 \text{ M}$; $K_L = 10^4$ at $I=0.025 \text{ M}$). In this approach, we ignore the Eu exchange reactions at high ionic strength (i.e. $I=0.5 \text{ M}$). Therefore, the value of $36 \pm 5 \text{ } \mu\text{mol/m}^2$ obtained for the $>\text{SOH}$ site density may be somewhat overestimated. In a second step, we interpret the PO_4 sorption isotherm in terms of $>\text{SOH}$ site density. In contrast to Eu, phosphate sorption is independent of ionic strength. Previous studies have shown that phosphate forms inner-sphere complexes at the iron oxide-aqueous interface (Tejedor-Tejedor and Anderson, 1990; Persson and Lovgren, 1996; Arai and Sparks, 2001). Similarly, strong binding of phosphate has been observed at silicate surfaces (Edzwald *et al.*, 1976). By analogy with these studies, we expect that phosphate should be complexed at specific sites (i.e. $>\text{SOH}$) of the basalt surface. PO_4 isotherms are interpreted here in this sense. Phosphate binding on goethite has been often interpreted as bidentate (Tejedor-Tejedor and Anderson, 1990). However, more recent studies suggest that a monodentate species may predominate at $\text{pH}<8$ and high surface loadings (Persson *et al.*, 1996; Kwon and Kubicki, 2004; Rahnemaie *et al.*, 2007). Since our study on basalt was conducted at $\text{pH}<8$ and high phosphate concentrations, we adopt the monodentate binding hypothesis. Using the one-site Langmuir equation (eq. 1), we obtain a site density of $30 \pm 5 \text{ } \mu\text{mol/m}^2$ (i.e. $5.4 \pm 0.9 \times 10^{-5} \text{ mol/g}$) (Fig 3A), which is close to the value determined for Eu at $I=0.5 \text{ M}$ (i.e. $36 \pm 5 \text{ } \mu\text{mol/m}^2$). In principle, Eu(III) and PO_4 may not “see” exactly the same $>\text{SOH}$ sites, since, under the pH conditions in our experiments, the former is a cation and the latter an anion. However, the closeness of the $[>\text{SOH}]$ values obtained with the Eu and PO_4 isotherms suggests that the reactive $>\text{SOH}$ sites are the same in both cases and that the experiments yield a relatively good estimate of their densities. Table 2 reports details of site densities and Langmuir constants for both phosphate and europium sorption experiments. In a third step, we consider total site density. At low ionic strength, Eu sorption is expected to reflect the total site density. Indeed, the value obtained (50

$\pm 6 \mu\text{mol/m}^2$) is close to the independently measured CEC ($52 \mu\text{mol/m}^2$). Combining the density data for specific and exchange sites, and selecting the most reliable values, we can propose a site distribution of $[>\text{SOH}]_{\text{TOT}}=30 \pm 5 \mu\text{mol/m}^2$ and $[>\text{XNa}]_{\text{TOT}}=22 \pm 5 \mu\text{mol/m}^2$ for Eu. The $>\text{SOH}$ concentration of our basalt sample is higher than the value generally given for simple oxides (3 to $8 \mu\text{mol/m}^2$ for quartz, Abendroth, 1970, Davis *et al.*, 1998; 4 to $17 \mu\text{mol/m}^2$ for goethite, Huang, 1996, Davis *et al.*, 1998, Villalobos and Leckie, 2001; $18 \mu\text{mol/m}^2$ for amorphous iron oxyhydroxide, Davis and Leckie, 1978), but it is close to the densities found for aluminosilicate surfaces (26 to $35 \mu\text{mol/m}^2$ for albite, Blum and Lasaga, 1991; $30 \mu\text{mol/m}^2$ for a chrysotile, Bales and Morgan, 1985). Few published values are available for more complex mineralogical assemblages. Payne *et al.* (2004) propose values of 0.2 to $20 \mu\text{mol/m}^2$ for shales based on different methods. The site densities obtained here by different approaches show perfect internal consistency, yielding a reliable value that corresponds well with the concentration of $>\text{SOH}=30 \mu\text{mol/m}^2$ given in the literature on aluminosilicates. We consider that it correctly reflects the surface composition of the basalt, which is likely dominated by feldspar, pyroxene and clays.

Surface complexation model:

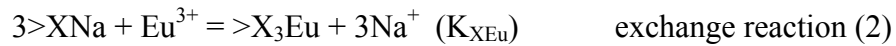
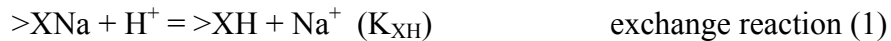
The basaltic surface is composed of a complex mixture of hydroxyl reaction sites. At least three different $>\text{SOH}$ groups are expected at the surface: $>\text{SiOH}$, $>\text{AlOH}$ and $>\text{FeOH}$. The cations Ca, Mg, Na and K are likely to be leached out from the surface during the first stage of interaction with water and therefore may not provide any surface sites. A reduction in the variety of surface sites during weathering is supported by many experimental studies (Lasaga and Blum, 1986; Gislason and Eugster, 1987; Blum and Lasaga, 1988; Gislason and Arnorsson, 1993; Stumm and Wollast, 1990), which suggest the formation of leached layers at the silicate surface, thus essentially restricting the reactive complexation sites to silanols and aluminols, as observed at clay surfaces. Each of these functional groups has acid/base properties, i.e. their own protonation and deprotonation constants, as well as specific constants for the REE interaction. Following the concept of the “Generalised Composite Approach” (Davis *et al.*, 1998 and 2004), we merged these sites into a single generic site because it would not appear feasible to quantify or characterize the specific site types for a complex rock such as basalt. The approximation of considering only one generic $>\text{SOH}$ site was also made by Wanner *et al.* (1994), Sverjensky and Sahai (1996) and El Aamrani *et al.*

(2002) in studies dealing with complex silicate mineral surfaces. For the generic site, we determined only REE sorption constants. Ideally, the determination of average proton affinity properties for the basalt solid surface could have been obtained by interpretation of acid/base titrations. However, preliminary simulations taking the acid/base constants of ferrinol, silanol or aluminol sites as given in the literature (Sverjensky and Sahai, 1996), have shown that, while the acid/base constants in each case slightly modified the best-fit value of the Eu sorption constants, they did not in any way improve the prediction of Eu sorption in our experimental batch system. Because surface acid/base reactions and REE sorption are interdependent, it is possible to describe them by a single reaction. However, we should bear in mind that this simplification gives rise to apparent sorption constants and apparent reaction stoichiometries.

To keep the number of adjustable parameters to a minimum, our model does not take into account the proton affinity constants. Davis *et al.* (1998, 2004) similarly ignored surface protonation in their studies on Zn and U(VI) sorption in sediments.

In contrast with the >SOH sites, we explicitly consider proton sorption at >XNa sites. Proton exchange is effective at low pH and low ionic strength (i.e. 0.025 M), and is responsible for a decrease of cation uptake at clay surfaces below pH 2-3. Exchange constants with $\log K_{XH}$ values from -3 to 0 have been proposed in the literature, with an average value of -1 (Fletcher and Sposito, 1989; Avena and De Pauli, 1998; Tournassat *et al.*, 2004; Gaucher *et al.*, 2006). Therefore, since we had no other constraint about the Na/H exchange reaction, we fixed $\log K_{XH} = -1$.

Finally, we included the following surface reactions in our model:



In our surface complexation model, we rule out electrostatic contributions to the surface reactions. This simplification has been suggested by several authors working on complex systems (Westall *et al.*, 1995; Davis *et al.*, 1998; Marmier and Fromage, 1999; Bradbury and Baeyens, 1997) and is a necessary consequence of ignoring surface protonation. It is acceptable in the case of moderately and strongly adsorbing ions such as REE at >SOH sites, where chemical forces are driving the interaction (Davis and Kent, 1990). For weakly adsorbing ions, where electrostatic contributions would be non-negligible, our model makes use of the ion exchange formalism.

The model is implemented with the CHESS[®] computer code. We use the >SOH and >XNa site densities determined above (Table 3). The reaction constants (i.e. K_{XEu} and K_{SOEu}) are adjusted to obtain the best fit of the Eu sorption data acquired as a function of pH, ionic strength and aqueous europium concentration. The fitted values are reported in Table 3. In Figure 4, the modeled isotherms and sorption edges are compared to the experimental data.

Although the aqueous carbonate complexes (i.e. $EuCO_3^+$) are taken into account in the aqueous model and are predominant between pH 7 and 8 (see artifacts section), we do not consider a specific sorption reaction for these species. As a result, the calculated sorption envelope decreases when $pH > 7$ (see figure 4A), which is not in accord with the experimental data. Determination of $EuCO_3^+$ sorption constants would have required a great deal of detailed experimental work at high pH. Because this reaction is at the margin of our study, it was discounted. At the opposite end of the pH range, the decrease of REE sorption at $pH < 3$ is well reproduced by the Na^+/H^+ exchange reaction and the associated decrease in >XNa site density.

In a second step, we consider the sorption data of the remaining 13 REE. Since no fractionation is observed at low ionic strength where cation exchange dominates the surface reactions, we assume the exchange constant to be the same for all the lanthanides. The fractionation of the REE pattern observed at high ionic strength and circumneutral pH implies that the complexation constant varies with the atomic number of the element. Thus, the NEM surface complexation constants are adjusted to yield the best description of the experimental data. Figure 5 shows the experimental and modeled sorption edges of four representative lanthanides (La, Nd, Dy and Yb) at $I = 0.5$ M. The fitted complexation constants vary only slightly from one lanthanide to another (from $\log K_{SOLa} = -1.15$ to $\log K_{SOLu} = -0.4$). The small but progressive shift reflects the fractionation in REE sorption, which is clearly observed in the near-neutral pH region. Such a fractionation in surface complexation of the REE has been recently recognized for other minerals, notably for amorphous ferric hydroxide (Quinn *et al.*, 2006a) and for natural sand (Tang and Johannesson, 2005).

In a third step, to validate the model as a predictive tool, we investigate competitive sorption between the 14 REE when concentrations are high (up to 10^{-4} mol/L at sorption equilibrium). Model calculations (Fig.6) indicate that, at pH 5.6, Eu sorption is lowered when all REE have high concentrations. This effect is observed to the same extent at high and low ionic strength, which suggests that the model reflects competition at surface complexation sites. The model provides a good description of the sorption experiments conducted at high concentrations of all REE, where we

would expect competition for sorption sites (Fig.7). We can thus conclude that the model may be satisfactorily used for data prediction.

Model application:

The general component approach allows us to describe the main features of REE retention by basalt, i.e. pH and ionic strength effects, fractionation of the pattern at high ionic strength and competition between the 14 REE at high concentrations (aqueous concentrations above 10^{-6} mol/L). We attain good agreement between experimental and modeling data by describing two types of surface reactions, one with exchange and the other with surface complexation, whereby the corresponding site densities are determined by independent experimental methods.

So far, we have not tested the robustness of the model when applied to other aluminosilicate mineral mixtures. As we did not have access to comparable sorption data on other basaltic samples, we applied the model to clay mineral samples for which REE sorption data have been published by Coppin *et al.* (2002) and Tertre *et al.* (2005). In their studies, the authors present sorption results in terms of distribution coefficients (i.e. K_d), expressed in mL/g, and defined as following:

$$K_d = \frac{V}{M} \times \frac{(C_i - C_f)}{C_f}$$
 where V and M are the volume of solution (mL) and the mass of solid (g),

respectively, and where C_i and C_f denote the initial and final aqueous concentrations of trace elements.

Using the sorption site densities determined specifically for the kaolinite and montmorillonite clay systems by Tertre *et al.* (2006a), we calculated the sorption envelop of Eu as a function of pH at I = 0.025 and 0.5 M (NaCl) using the GC model with the constants determined in the present study and the surface area reported in studies on clays (the only imported parameter). Figure 8 show that experimental data of Eu sorption by kaolinite (data from Coppin *et al.*, 2002) are well described by the sorption envelope predicted by the “basalt”-GC model, used without further adjustment. Predictions of our model are expressed in terms of percent sorption (Fig. 8A) and log K_d (Fig 8B). The K_d approach helps in validating the model at both low and high surface-area coverage. Indeed, the model cannot be validated merely by the satisfactory prediction of attainment of 100% sorption (Fig. 8A, data for low ionic strength). On the other hand, the K_d is sensitive to slight variations in surface and solution concentrations and is therefore a reliable parameter for assessing a sorption model.

Other predictions for montmorillonite (not shown here) are similarly of good quality. For both minerals, we note that, at pH=4-5 and high ionic strength, the predicted values are slightly lower (<10%) than the experimental results. This effect may be due to multiple-exchange sites present on the clay surfaces that are not included in the present model. Apart from this difference, the model results are in good agreement with the experimental data of both clay minerals. Moreover, the values predicted by our GC model are in agreement with those calculated by more sophisticated electrostatic models for pure clays. This suggests that the minor clay fraction in the basalt contributes greatly to the REE retention properties, and that the general composite approach is an easy and efficient tool for describing sorption by complex mineral assemblages.

ACKNOWLEDGEMENTS

The authors would like to thank J. Tang, J. Schijf, R. Byrne and one anonymous reviewer for their substantial contributions to improving the paper. We would like to thank A. Fischer for the basalt samples. We are also grateful to R. Freydier and F. Candaudap for their assistance in ICP-MS at Toulouse University, J.F. Barthe for his help in phosphorus analyses at Lille University and F. Villiéras for the CEC measurement performed at LEM in Nancy. M.S.N. Carpenter post-edited the English style.

Associate editor: R. Byrne.

REFERENCES

- Abendroth R. P., 1970 Behaviour of a pyrogenic silica in simple electrolytes. *J. Colloid Interface Sci.* **34**, 591–596.
- Akagi T., Shabani M.B. and Masuda A., 1993 Lanthanide tetrad effect in kimuraite [CaY₂(CO₃)₄.6H₂O]: Implication for a new geochemical index. *Geochim. Cosmochim. Acta* **57**, 2899-2905.

APHA, AWWA and WPCF, 1998 Standards methods for the examination water and wastewater. American public health association, Washington, DC, p 456.

Arai Y. and Sparks D.L., 2001 ATR-FTIR Spectroscopic investigation on phosphate adsorption mechanisms at the ferrihydrite-water interface. *J. Colloid Interface Sci.* **241**, 317-326.

Avena M.J. and De Pauli C.P, 1998 Proton adsorption and electrokinetics of an Argentinean montmorillonite. *J. Colloid Interface Sci.* **202**, 195-204.

Bales R.C. and Morgan J.J., 1985 Dissolution kinetics of chrysotyle at pH 7 to 10. *Geochim. Cosmochim. Acta* **49**, 2281-2288.

Balistrieri L.S., Brewer P.G. and Murray J.W., 1981 Scavenging residence times of trace metals and surface chemistry of sinking particles in the deep ocean. *Deep-Sea Res.* **28A**, 101-121.

Barnett M.O., Jardine P.M. and Brooks S.C., 2002 U(IV) adsorption to heterogeneous subsurface media: Application of a surface complexation model. *Environ. Sci. Technol.* **36**, 937-372.

Barrow N.J., Bowden J.W., Posner A.M. and Quirk, P.J., 1980 Describing the effects of electrolyte on adsorption of phosphate by a variable charge surface. *Aust. J. Soil. Res.* **18**, 395-404.

Bau M., Koschinsky A., Dulski P. and Hein J.R., 1996 Comparison of the partitioning behaviours of yttrium, rare earth elements, and titanium between hydrogenetic marine ferromanganese crusts and seawater. *Geochim. Cosmochim. Acta* **60**, 1709-1525.

Bau M., 1999 Scavenging of dissolved yttrium and rare earths by precipitating iron oxyhydroxide: Experimental evidence for Ce oxidation, Y-Ho fractionation, and lanthanide tetrad effect. *Geochim. Cosmochim. Acta* **63**, 67-77.

Blum A. and Lasaga A.C., 1988 Role of surface speciation in the low-temperature dissolution of minerals. *Geochim. Cosmochim. Acta* **55**, 2193-2201.

Blum A. and Lasaga A.C., 1991 Role of surface speciation in the dissolution of albite. *Nature* **331**, 421-433.

Bonnot-Courtois C. and Jaffrezic-Renault N., 1982 Etude des échanges entre terres rares et cations interfoliaires de deux argiles. *Clay Minerals* **17**, 409-420.

Bradbury M.H. and Baeyens B., 1997 A mechanistic description of Ni and Zn sorption on Namontmorillonite. Part II: modeling. *J. Contam. Hydro.* **27**, 223-248.

Bradbury M.H. and Baeyens B., 2002 Sorption of Eu on Na and Ca-montmorillonite: Experimental investigations and modeling with cation exchange and surface complexation. *Geochim. Cosmochim. Acta* **66**, 2325-2334.

Byrne R.H. and Kim K-H, 1990 Rare earth element scavenging in seawater. *Geochim. Cosmochim. Acta* **54**, 2645-2656.

Castet S., Dandurand J.L., Schott J. and Gout R. 1993 Boehmite solubility and aqueous aluminium speciation in hydrothermal solutions (90-350°C): experimental study and modeling. *Geochim. Cosmochim. Acta* **57**, 4869-4884.

Catalette H., Dumonceau J. and Ollar P., 1998 Sorption of cesium, barium and europium on magnetite. *J. Contam. Hydro.* **35**, 151-159.

Coppin F., Berger G., Bauer A., Castet S. and Loubet M., 2002 Sorption of lanthanides on smectite and kaolinite. *Chem. Geol.* **182**, 57-68.

Davis J.A. and Leckie J.O., 1978 Surface ionization and complexation at the oxide/water interface. II Surface properties of amorphous iron oxyhydroxide and adsorption of metal ions. *J. Colloid Interface Sci.* **67**, 90-107.

Davis J.A. and Kent D.B., 1990 Surface complexation modeling in aqueous geochemistry: mineral-water interface geochemistry. *Rev. Mineral* **23**, 177-260.

Davis J.A., Coston J.A., Kent D.B. and Fuller C.C., 1998 Application of the surface complexation concept to complex mineral assemblages. *Environ. Sci. Technol.* **32**, 2820-2828.

Davis J.A., Meece D.E., Kohler M. and Curtis G.P., 2004 Approaches to surface complexation modeling of Uranium (VI) adsorption on aquifer sediments. *Geochim. Cosmochim. Acta* **68**, 3621-3641.

Davranche M., Pourret O., Gruau G. and Dia A., 2004 Impact of humate complexation on the adsorption of REE onto Fe oxyhydroxide. *J. Colloid Interface Sci.* **277**, 271-279.

Davranche M., Pourret O., Gruau G., Dia A. and Le Coz-Bouhnik M., 2005 Adsorption of REE(III)-humate complexes onto MnO₂: Experimental evidence for cerium anomaly and lanthanide tetrad effect suppression. *Geochim. Cosmochim. Acta* **69**, 4825-4835.

De Carlo E.H., Wen X.Y. and Irving M., 1998 The influence of redox reactions on the uptake of dissolved Ce by suspended Fe and Mn oxide particles. *Aquat. Geochem.* **3**, 357-389.

Edzwald J.K., Toensing D.C. and Leung M.C., 1976 Phosphate adsorption reactions with clay minerals. *Environ. Sci. Technol.* **10**, 485-490.

El Aamrani F.Z., Duro L., De Pablo J. and Bruno J., 2002 Experimental study and modeling of the sorption of uranium (VI) onto olivine-rock. *Applied Geochem.* **17**, 399-408.

Fischer A., 2004 Etude des Améthystes des Basaltes du Bassin de Parana (Brésil) et sa contribution pour leur genèse. PhD Thesis, Porto Alegre.

Fletcher P. and Sposito G., 1989 The chemical modeling of clay/electrolyte interactions for montmorillonite. *Clay Miner.* **24**, 375-391.

Gaucher E.C., Blanc P., Bardot F., Braibant G., Buschaert S., Crouzet C., Gautier A., Girard J.P., Jacquot E., Lassin A., 2006 Modelling the porewater chemistry of the Callovian-Oxfordian formation at a regional scale. *Comptes Rendus Geosciences* **338**, 917-930.

Gislason S.R. and Eugster H.P., 1987 Meteoric water-basalt interactions. I: A laboratory study. *Geochim. Cosmochim. Acta* **51**, 2827-2840.

Gislason S.R. and Arnorsson S., 1993 Dissolution of primary basaltic minerals in natural waters: saturation state and kinetics. *Chem. Geol.* **105**, 117-135.

Gomes MEB, 1996 Mecanismos de resfriamento, estruturação e processos pós-magmáticos em basaltos da Bacia do Paraná - Região de Frederico Westphalen (RS), Brasil. PhD Thesis, Porto Alegre.

Hayes K.F. and Leckie J.O., 1987 Modeling ionic strength effect on cation adsorption at hydrous oxide/solution interfaces. *J. Colloid Interface Sci.* **115**, 564-572.

Helgeson H.C., Kirkham D.H. and Flowers G.C. 1981 Theoretical prediction of the thermodynamic behaviour of aqueous electrolytes at high pressures and temperature; IV. calculation of the activity coefficients, osmotic coefficients and apparent molal standard and relative partial molal properties to 600°C and 5 kb. *Am. J. Sc.* **281**, 1249-1516.

Huang C.P. and Stumm W., 1973 Specific adsorption of cations on hydrous γ -Al₂O₃. *J. Colloid Interface Sci.* **43**, 409-420.

Huang P., 1996 The effects of the adsorption of metal ions and surfactant behaviour on the interfacial behaviour of silicate minerals. Ph.D. thesis, University of California, Berkeley.

Irber W., 1999 The lanthanide tetrad effect and its correlation with K/Rb, Eu/Eu*, Sr/Eu, Y/Ho and Zr/Hf of evolving peraluminous granite suites. *Geochim. Cosmochim. Acta* **63**, 489-508.

Johnson J.W., Oelkers E.H. and Helgeson H.C., 1992 SUPCRT92: A software package for calculating the standard molar thermodynamic properties of minerals; gases, aqueous species and reactions from 1 to 5000 bars and 0 to 1000°C. *Computer Geosci.* **18**, 899-947.

Kagi H., Dohmoto Y., Takano S. and Masuda A., 1993 Tetrad effect in lanthanide partitioning between calcium sulfate crystal and its saturated solution. *Chem. Geol.* **107**, 71-82.

Kawabe I., Kitahara T. and Naito K., 1991 Non-chondritic yttrium/holmium ratio and lanthanide tetrad effect observed in pre-Cenozoic limestones. *Geochem. J.* **25**, 31-44.

Kawabe I., 1992 Lanthanide tetrad effect in the Ln³⁺ ionic-radii and refined spin-pairing energy theory. *Geochem. J.* **26**, 309-335.

Kawabe I., 1995 Tetrad effects and fine structures of REE abundance patterns of granitic and rhyolitic rocks: ICP-AES determinations of REE and Y in eight GSJ reference rocks. *Geochem. J.* **29**, 213-230.

Kawabe I., Ohta A., Ishii S., Tokumura M. and Miyauchi K., 1999 REE partitioning between Fe-Mn oxyhydroxide precipitates and weakly acid NaCl solutions: Convex tetrad effect and fractionation of Y and Sc from heavy lanthanides. *Geochem. J.* **33**, 167-179.

Klungness G.D. and Byrne R. H., 2000 Comparative hydrolysis behavior of the rare earths and yttrium: the influence of temperature and ionic strength. *Polydron* **19**, 99-107.

Koepfenkastro D. and De Carlo E.H., 1992 Sorption of rare earth elements from seawater onto synthetic mineral particles: An experimental approach. *Chem. Geol.* **95**, 251-263.

Kosmulski, M., 1997 Adsorption of Trivalent Cations on Silica. *J. Colloid Interface Sci.* **195**, 395-403.

Kowal-Fouchard A., 2002 Etude des mécanismes de rétention des ions U(IV) et Eu(III) sur les argiles : influence des silicates. Ph. D. Thesis, Université Paris Sud, France, 330p.

Kowal-Fouchard A., Drot R., Simoni E., Marmier N., Fromage F. and Ehrhardt J.J., 2004 Structural identification of europium(III) adsorption complexes on montmorillonite. *New. J. Chem.* **28**, 864-869.

Kulik D.A., Aja S.U., Sinitsyn V.A. and Wood S.A., 2000 Acid-base surface chemistry and sorption of some lanthanides on K⁺-saturated Marblehead illite: II. A multisite-surface complexation modelling. *Geochim. Cosmochim. Acta* **64**, 195-213.

Kwon, K. and Kubicki, J. D. 2004 Molecular orbital theory study on surface complex structures of phosphates to iron hydroxides: Calculation of vibrational frequencies and adsorption energies. *Langmuir* **20**, 9249-9254.

Lasaga A.C. and Blum A.E., 1986 Surface chemistry, etch pits and mineral-water reactions. *Geochim. Cosmochim. Acta* **50**, 2363-2379.

Lauber M., Baeyens B. and Bradbury M.H., 2000 Physico-Chemical characterisation and sorption measurements of Cs, Sr, Ni, Eu, Th, Sn and Se on OPALINUS CLAY from Mont Terri. Nagra Technical Report NTB 00-11, 78p.

Lee S.G., Masuda A. and Kim H.S., 1994 An early Proterozoic leuco-granitic gneiss with the REE tetrad phenomenon. *Chem. Geol.* **114**, 59-67.

Luo Y-R and Byrne R.H., 2004 Carbonate Complexation of Yttrium and Rare Earth Elements in Natural Waters. *Geochim. Cosmochim. Acta* **68**, 691-699.

Lützenkirchen J., 1997 Ionic strength effects on cation sorption to oxides: Macroscopic observations and their significance in microscopic interpretation. *J. Colloid Interface Sci.* **195**, 149-155.

Marmier N., 1994 Etude expérimentale et modélisation de la fixation d'éléments en trace sur des oxydes minéraux - Contribution à l'étude des propriétés adsorbantes des solides naturels. Ph. D. Thesis, Université Reims Champagne-Ardenne, France.

Marmier N., Dumonceau J. and Fromage F., 1997 Surface complexation modeling of Yb(III) sorption and desorption on hematite and alumina. *J. Contam. Hydro.* **26**, 159-167.

Marmier N. and Fromage F., 1999 Comparing electrostatic and nonelectrostatic surface complexation modeling of the sorption of lanthanum on hematite. *J. Colloid Interface Sci.* **212**, 252-263.

Masuda A. and Akagi T., 1989 Lanthanide tetrad effect observed in leucogranites from China. *Geochem. J.* **23**, 245-253.

McLennan S.M., 1994 Rare earth element geochemistry and the “tetrad” effect. *Geochim. Cosmochim. Acta* **58**, 2025-2033.

Meier L. P. and Kahr G., 1999 Determination of the cation exchange capacity (CEC) of clay minerals using the complexes of copper (II) ion with triethylenetetramine and tetraethylenepentamine. *Clays Clay Miner.* **47**, 386-388.

Monecke T., Kempe U., Monecke J., Sala M. and Wolf D., 2002 Tetrad effect in rare earth element distribution patterns: a method of quantification with application to rock and mineral samples from granite-related rare metal deposits. *Geochim. Cosmochim. Acta* **66**, 1185-1196.

Monecke T., Kempe U. and Monecke J., 2003 Comment on the paper “W- and M-type tetrad effects in REE patterns for water-rock systems in the Tono uranium deposit, central Japan” by Takahashi Y., Yoshida H., Sato N., Hama K., Yusa Y. and Shimizu H. *Chem. Geol.* **202**, 183-184.

Muecke G.K. and Möller P., 1988 The not-so rare earths. *Sci. Amer.* **258**, 72-77.

Naveau A., Monteil-Rivera F., Dumonceau J. and Boudesocque S., 2005 Sorption of europium on a goethite surface: influence of background electrolyte. *J. Contam. Hydro.* **77**, 1-16.

Ohta A. and Kawabe I., 2001 REE (III) adsorption onto Mn dioxide (δ -MnO₂) and Fe oxyhydroxide: Ce (III) oxidation by δ -MnO₂. *Geochim. Cosmochim. Acta* **65**, 695–703.

Parkhurst D.L., 1995 User’s guide to PHREEQC-A computer program for speciation, reaction-path, advective-transport, and inverse geochemical calculations. 95-4227. U.S. Geological Survey, Lakewood, CO.

Payne T.E., Davis A.D., Ochs M., Olin M. and Tweed C.J., 2004 Uranium adsorption on weathered schist – intercomparison of modeling approaches. *Radiochim. Acta* **92**, 651-661.

Persson P. and Lovgren L., 1996 Potentiometric and spectroscopic studies of sulphate complexation at the goethite-water interface. *Geochim. Cosmochim. Acta* **60**, 2789-2799.

Persson P., Nilsson N. and Sjöberg S., 1996 Structure and bonding of orthophosphate ions at the iron oxide-aqueous interface. *J. Colloid Interface Sci.* **177**, 263-275.

Quinn K.A., Byrne R.H. and Schijf J., 2004 Comparative scavenging of Yttrium and the rare earth elements in seawater: competitive influences of solution and surface chemistry. *Aquat. Geochem.* **10**, 59-80.

Quinn K.A., Byrne R.H. and Schijf J., 2006a Sorption of yttrium and rare earth elements by amorphous ferric hydroxide: Influence of pH and ionic strength. *Mar. Chem.* **99**, 128-150.

Quinn K.A., Byrne R.H. and Schijf J., 2006b Sorption of yttrium and rare earth elements by amorphous ferric hydroxide: Influence of solution complexation with carbonate. *Geochim. Cosmochim. Acta* **70**, 4151-4165.

Rabung T., Stumpf T., Geckeis H., Klenze R. and Kim J. I., 2000 Sorption of Am(III) and Eu(III) onto γ -alumina: experiment and modeling. *Radiochim. Acta* **88**, 711-716.

Rabung T., Pierret M. C., Bauer A., Geckeis H., Bradbury M. H. and Baeyens B., 2005 Sorption of Eu(III)/Cm(III) on Ca-montmorillonite and Na-illite. Part 1: Batch sorption and time-resolved laser fluorescence spectroscopy experiments. *Geochim. Cosmochim. Acta* **69**, 5393-5402.

Rahnemaie R., Hiemstra T. and van Riemsdijk W. H., 2007 Geometry, charge distribution, and surface speciation of phosphate on goethite. *Langmuir* **23**, 3680-3689.

Ruaya J.R. and Seward T.M. 1987 The ion-pair constant and other thermodynamic properties of HCl up to 350°C. *Geochim. Cosmochim. Acta* **51**, 121-130.

Schenato F., Formoso M.L.L., Dudoignon P., Meunier A., Proust D., Mas A., 2003 Alteration processes of a thick basaltic lava flow of the Paraná Basin (Brazil): petrographic and mineralogical studies. *J South American Earth Sciences* **16**, 423-444.

Scopel R.M., 1997 Estudo dos derrames basálticos portadores de ametista da região de Ametista do Sul, RS - Brasil. Alteração pós-magmática. PhD Thesis, Porto Alegre.

Shannon R.D., 1976 Revised effective radii and systematic studies of interatomic distances in halides and chalcogenides. *Acta. Cryst.* **A32**, 751-767.

Sholkovitz E.R., Landing W.M. and Lewis B.L., 1994 Ocean particle chemistry: The fractionation of rare earth elements between suspended particles and seawater. *Geochim. Cosmochim. Acta* **58**, 1567-1579.

Sinitsyn, V.A., Aja, S.U., Kulik, D.A., Wood, S.A., 2000. Acid-base surface chemistry and sorption of some lanthanides on K⁺-saturated marblehead illite: I. Results of an experimental investigation. *Geochim. Cosmochim. Acta* **64**, 185–194.

Stumm W. and Wollast R., 1990 Coordination chemistry of Weathering: Kinetics of the surface-controlled dissolution of oxide minerals. *Rew. Geophys.* **28**, 53-69.

Stumpf, T., Rabung, T., Klenze, R., Geckeis, H. and Kim, J.-I., 2001 Spectroscopic study of Cm (III) Sorption onto Y-Alumina. *J. Colloid Interface Sci.* **238**, 219-224.

Stumpf T., Bauer A., Coppin F., Fanghanel T. and Kim J. I., 2002 Inner-sphere, outer-sphere and ternary surface complexes: a TRLFS study of the sorption process of Eu(III) onto smectite and kaolinite. *Radiochim. Acta* **90**, 345-349.

Stumpf T., Hennig C., Bauer A., Denecke M. A. and Fanghanel T., 2004 An EXAFS and TRLFS study of the sorption of trivalent actinides onto smectite and kaolinite. *Radiochim. Acta* **92**, 133-138.

Sverjensky D.A. and Sahai N., 1996 Theoretical prediction of single-site surface-protonation equilibrium constants for oxides and silicates in water. *Geochim. Cosmochim. Acta* **60**, 3773-3797.

Takahashi Y., Yoshida H., Sato N., Hama K., Yusa Y. and Shimizu H., 2002 W- and M-type tetrad effects in REE patterns for water-rock systems in the Tono uranium deposit, central Japan. *Chem. Geol.* **184**, 311-335.

Tang J. and Johannesson K.H., 2005 Adsorption of rare earth elements onto Carrizo sand: Experimental investigations and modeling with surface complexation. *Geochim. Cosmochim. Acta* **69**, 5247-5261.

Tanger J.C. and Helgeson H.C. 1997 Revised equation of state for the standard partial molal properties of ions and electrolytes. *Am. J. Sc.* **288**, 19-98.

Tao Z., Wang X., Guo Z. and Chi T., 2004 Is there a tetrad effect in the adsorption of lanthanides (III) at solid-water interfaces? *Colloids and Surfaces A: Physicochem. Eng. Aspects* **251**, 19-25.

Tejedor-Tejedor M.I. and Anderson M.A., 1990 Protonation of phosphate on the surface of goethite as studied by CIR-FTIR and electrophoretic mobility. *Langmuir* **6**, 602-611.

Tertre E., Berger G., Castet S., Loubet M. and Giffaut E., 2005 Experimental study of adsorption of Ni^{2+} , Cs^+ and Ln^{3+} onto Na-montmorillonite up to 150°C. *Geochim. Cosmochim. Acta* **69**, 4937-4948.

Tertre E., Castet S., Berger G., Loubet M. and Giffaut E., 2006a Acid-base surface chemistry of kaolinite and Na-montmorillonite in aqueous electrolyte solutions at 25 and 60°C: experimental study and modeling. *Geochim. Cosmochim. Acta* **70**, 4579-4599.

Tertre E., Berger G., Simoni E., Castet S., Giffaut E., Loubet M. and Catalette H., 2006b Europium retention onto clay minerals from 25 to 150°C: experimental measurements, spectroscopic features and sorption modeling. *Geochim. Cosmochim. Acta* **70**, 4563-4578.

Tournassat C., Neaman A., Villiéras F., Bosbach D. and Charlet L., 2003 Nanomorphology of montmorillonite particles: Estimation of the clay edge sorption site density by low-pressure gas adsorption and AFM observations. *Am. Mineral.* **88**, 1989-1995.

Tournassat C., Ferrage E., Poinson C. and Charlet L., 2004 The titration of clay minerals II. Structure-base model and implications for clay reactivity. *J. Colloid Interface Sci.* **273**, 238-250.

Wanner H., Albinson Y., Karnland O., Wieland E., Wersin P. and Charlet L., 1994 The acid/base chemistry of Montmorillonite. *Radiochim. Acta* **66/67**, 157-162.

Westall J.C., Jones J.D., Turner G.D. and Zachara J.M., 1995 Models for association of metal ions with heterogeneous environmental sorbents. 1. Complexation of Co(II) by Leonardite Humic Acid as a function of pH and NaClO₄ concentration. *Environ. Sci. Technol.* **29**, 951-959.

Villalobos M. and Leckie J.O., 2001 Surface complexation modeling of carbonate effects on the adsorption of Cr(III), Pb(II) and U(VI) on goethite. *Environ. Sci. Technol.* **35**, 3849-3856.

A

oxides	SiO ₂	Al ₂ O ₃	Fe ₂ O ₃	MnO	MgO	CaO	Na ₂ O	K ₂ O	TiO ₂	P ₂ O ₅
weight %	49.6	12.5	15.3	0.2	4.1	8.2	2.6	1.7	3.6	0.6

B

REE	La	Ce	Pr	Nd	Sm	Eu	Gd	Tb	Dy	Ho	Er	Tm	Yb	Lu
C (ppm)	36.6	81.7	10.1	42.0	8.1	2.8	8.3	1.4	7.8	1.5	4.1	0.6	3.6	0.5

Table 1: (A) Chemical composition and (B) REE concentrations of the basalt (Fischer, 2004).

Adsorbate	pH ± 0.2	Ionic strength (NaCl) in mol/L	Langmuir parameters	
			S _{max} (site density) in 10 ⁻⁵ mol/g	K _L (Langmuir constant) in L/mol
phosphate	4.7	0.025	5.4 ± 0.9	5.10 ³
phosphate	4.7	0.5	5.4 ± 0.9	5.10 ³
Eu(III)	5.6	0.025	9.0 ± 1.1	10 ⁴
Eu(III)	5.6	0.5	6.9 ± 1.1	2.10 ³

Table 2: Experimental conditions and Langmuir parameters (maximal site densities, sorption constants) for PO₄ and Eu(III) sorption.

Sorption reactions	log K (25°C)
$>XNa + H^+ = >XH + Na^+$	-1 ± 0.5
$3>XNa + Eu^{3+} = >X_3Eu + 3Na^+$	9.7 ± 0.3
$>SOH + Eu^{3+} = >SOEu^{2+} + H^+$	-0.5 ± 0.05

Total site densities (in $\mu\text{mol}/\text{m}^2$):

- $>XNa = 22$
- $>SOH = 30$

Table 3: Sorption reactions and corresponding sorption constants. Constants for Eu are obtained by fitting the GC model curves to the experimental data. The proton affinity constant for the exchange sites is taken from literature data, representing an average value valid for clay/water and shale/water systems (Fletcher and Sposito, 1989; Avena and De Pauli, 1998; Tournassat *et al.*, 2004; Gaucher *et al.*, 2006).

Sorption reactions	log K (25°C)
$>XNa + H^+ = >XH + Na^+$	-1 ± 0.5
$3>XNa + REE^{3+} = >X_3REE + 3Na^+$ with REE = La, Ce, Pr, Nd, Sm, Eu, Gd, Tb, Dy, Ho, Er, Tm, Yb and Lu.	9.7 ± 0.3
$>SOH + La^{3+} = >SOLa^{2+} + H^+$	-1.15 ± 0.05
$>SOH + Ce^{3+} = >SOCe^{2+} + H^+$	-1.0 ± 0.05
$>SOH + Pr^{3+} = >SOPr^{2+} + H^+$	-1.0 ± 0.05
$>SOH + Nd^{3+} = >SONd^{2+} + H^+$	-0.8 ± 0.05
$>SOH + Sm^{3+} = >SOSm^{2+} + H^+$	-0.55 ± 0.05
$>SOH + Eu^{3+} = >SOEu^{2+} + H^+$	-0.5 ± 0.05
$>SOH + Gd^{3+} = >SOGd^{2+} + H^+$	-0.5 ± 0.05
$>SOH + Tb^{3+} = >SOTb^{2+} + H^+$	-0.5 ± 0.05
$>SOH + Dy^{3+} = >SODy^{2+} + H^+$	-0.5 ± 0.05
$>SOH + Ho^{3+} = >SOHo^{2+} + H^+$	-0.45 ± 0.05
$>SOH + Er^{3+} = >SOEr^{2+} + H^+$	-0.4 ± 0.05
$>SOH + Tm^{3+} = >SOTm^{2+} + H^+$	-0.4 ± 0.05
$>SOH + Yb^{3+} = >SOYb^{2+} + H^+$	-0.4 ± 0.05
$>SOH + Lu^{3+} = >SOLu^{2+} + H^+$	-0.4 ± 0.05

Total site densities (in $\mu\text{mol}/\text{m}^2$):

- $>XNa = 22$
- $>SOH = 30$

Table 4: Sorption reactions and corresponding sorption constants. Constants for REE are obtained by fitting the GC model curves to the experimental data. For the proton affinity constant for the exchange sites, see Table 3 caption.

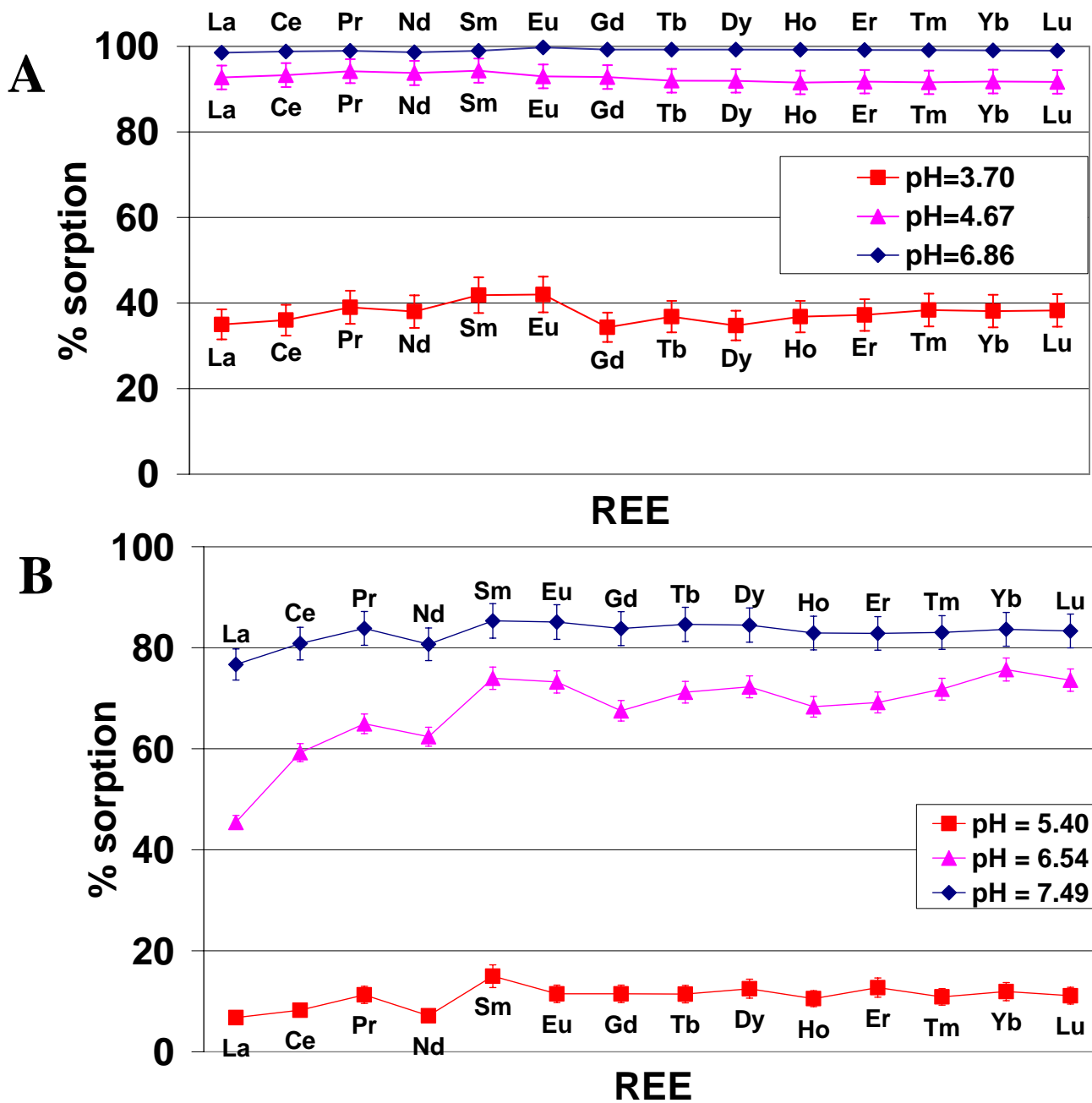


Figure 1: Extent of sorption (%) of the 14 lanthanides, at different pH and with NaCl concentrations of 0.025 M (A), and 0.5 M (B). Initial REE concentrations are 100 ppb for each lanthanide.

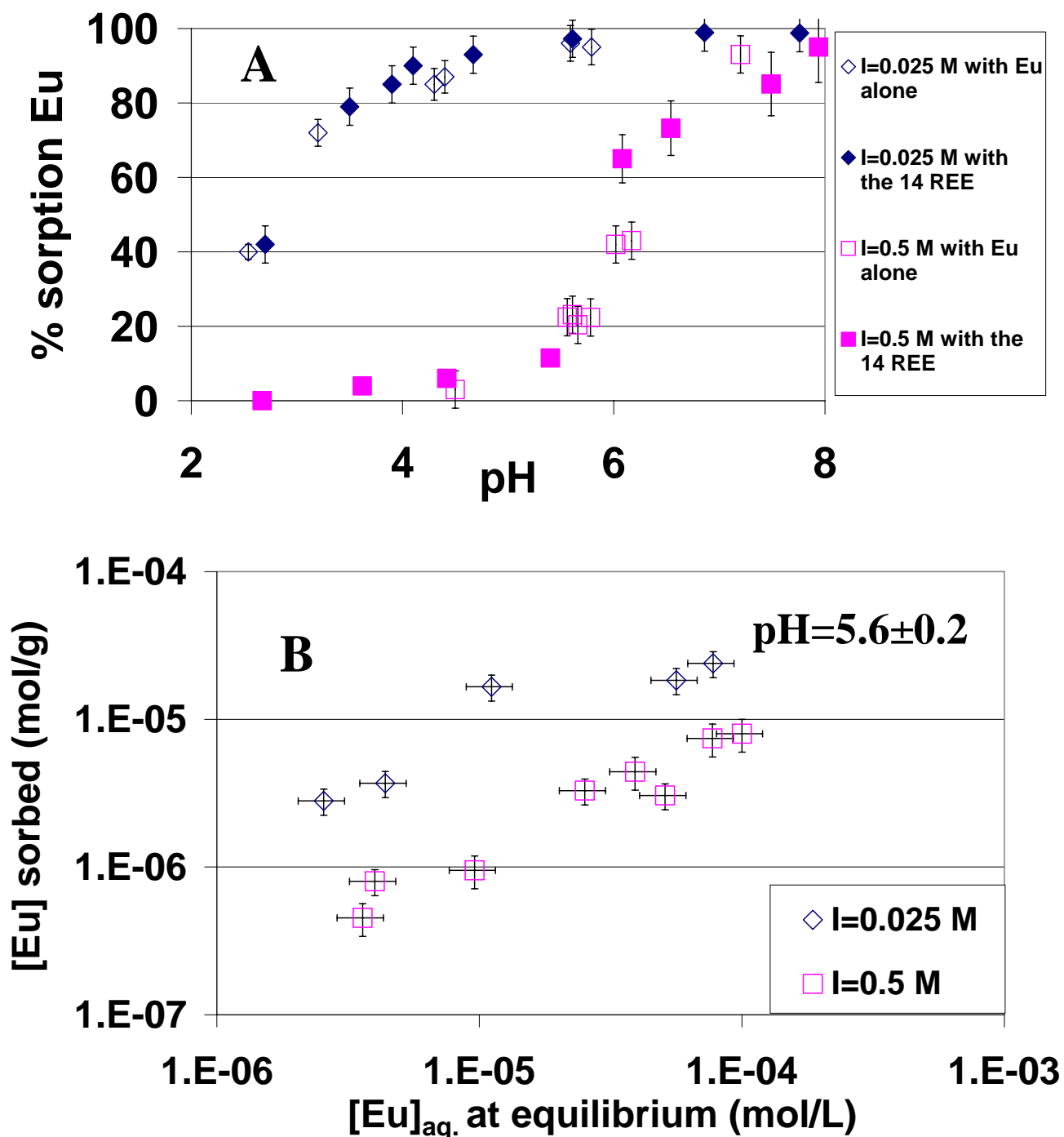


Figure 2:

(A) Europium sorbed by the basalt as a function of pH and ionic strength. Open symbols represent the system with only europium present ($[Eu]_{initial} = 100$ ppb), whereas solid symbols indicate experiments with all REE present ($[REE]_{initial} = 100$ ppb).

(B) Sorption isotherms for europium at two ionic strengths, at $pH=5.6\pm 0.2$. No other REE are present in the experiments.

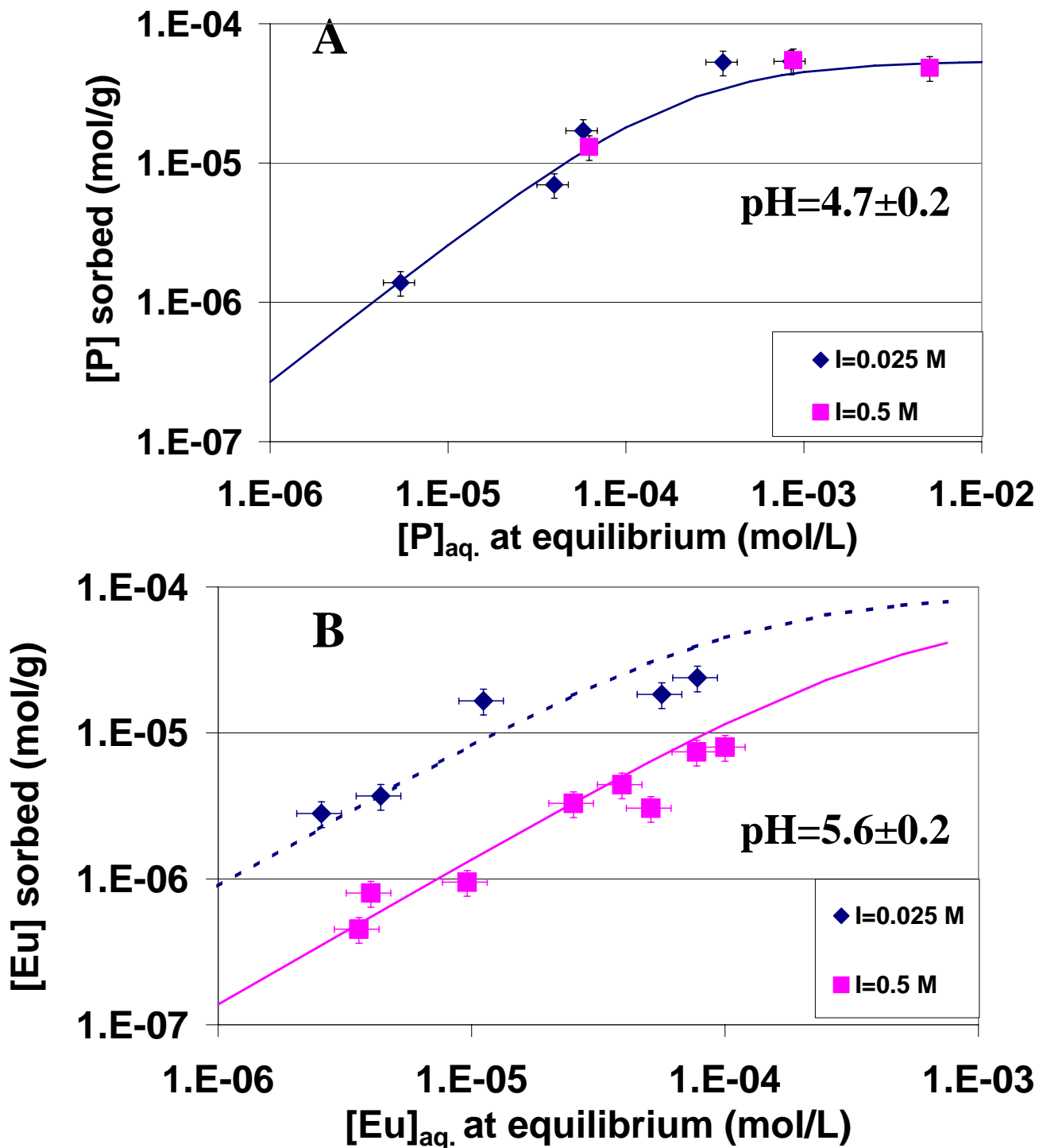


Figure 3: Experimental sorption data (symbols) as a function of aqueous equilibrium concentration shown for two ionic strengths, with corresponding Langmuir isotherms (solid line). A: Phosphate at $pH=4.7\pm 0.2$; B: Europium (no other REE present) at $pH=5.6\pm 0.2$ (same experimental data as in figure 2B).

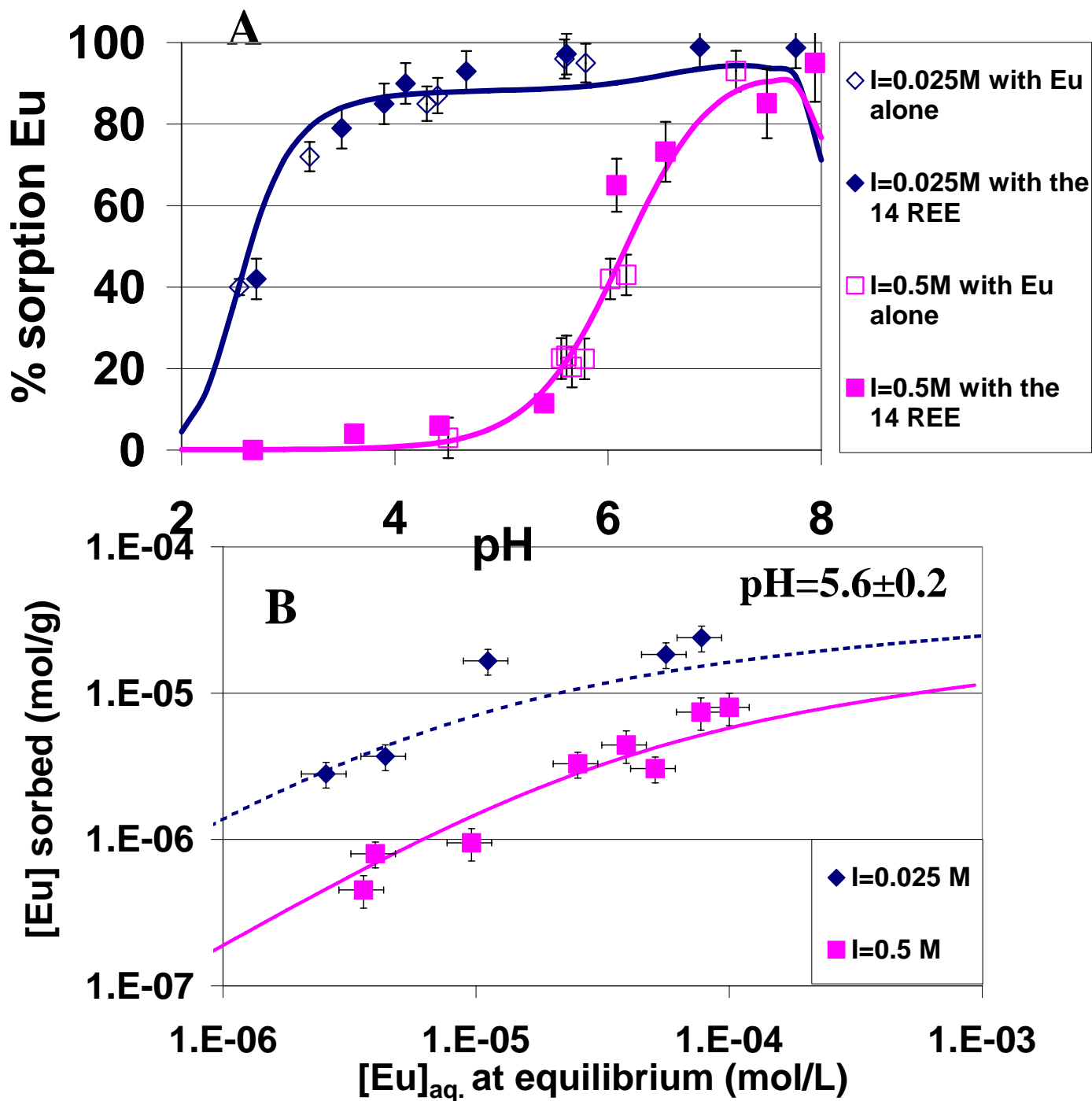


Figure 4: Experimental data as in Fig. 2. The solid lines indicate the Eu(III) sorption as predicted by the GC model.

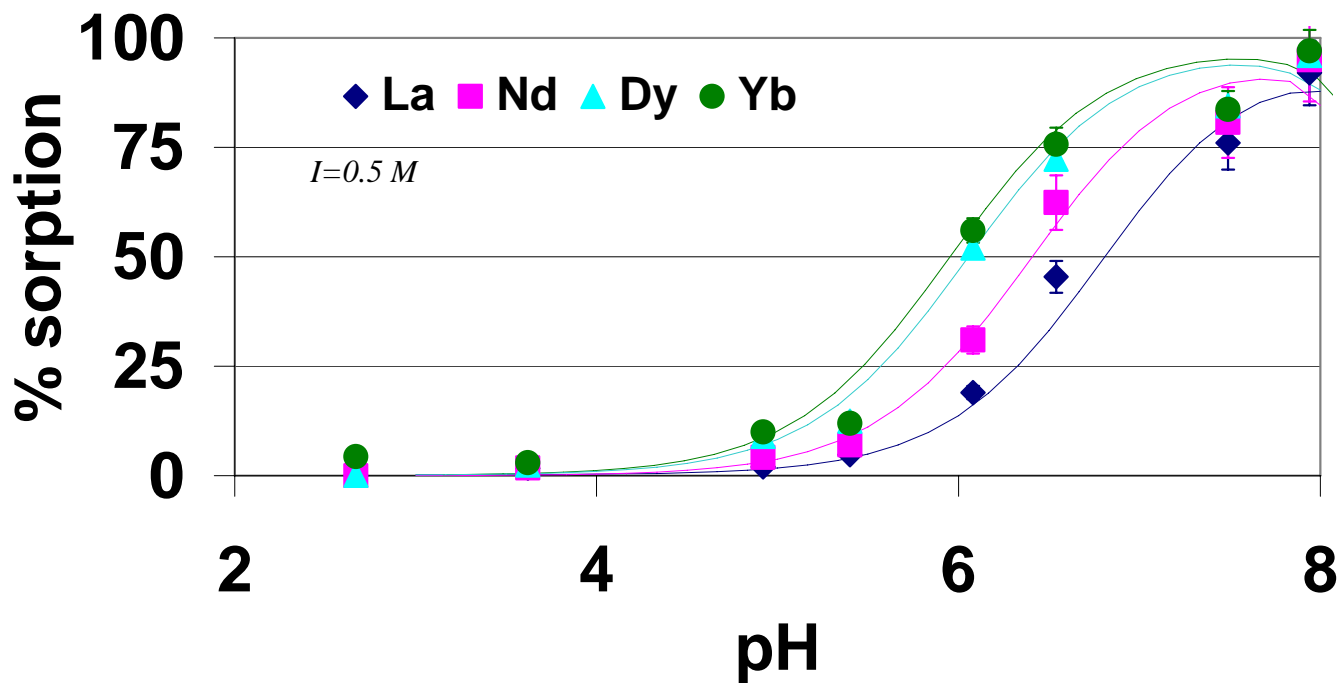


Figure 5: Extent of sorption (%) of La(III), Nd(III), Dy(III) and Yb(III) (symbols) on basalt as a function of pH, in 0.5 M NaCl solutions, and sorption curves (lines) predicted by the GC surface complexation model. $[REE]_{\text{initial}}$ for each REE=100 ppb.

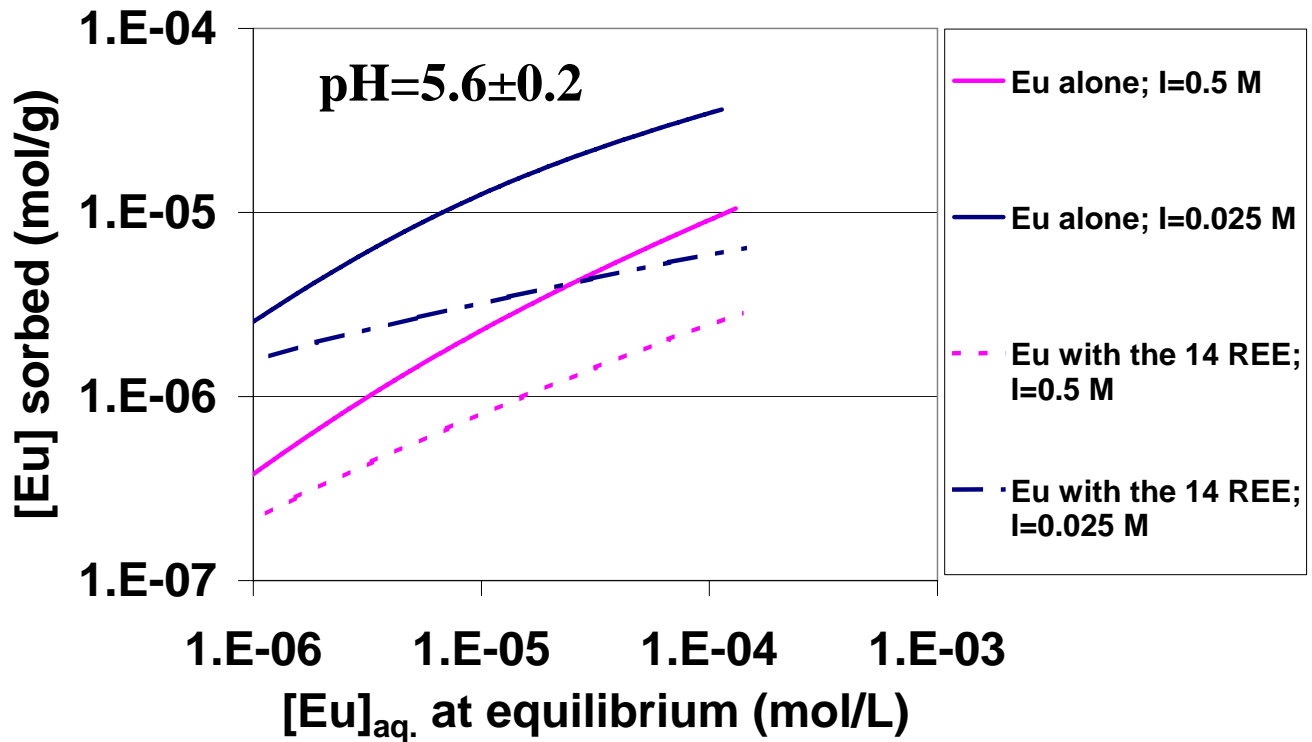


Figure 6: Europium isotherms calculated by the GC model in the presence of europium only (solid lines) and in the presence of all 14 REE (dashed lines).

Four simulations were performed at a constant pH of 5.6 and at two ionic strengths (0.025 and 0.5 M). Parameters of the models are presented in Table 4. $[\text{REE}]_{\text{initial}}$ for each REE varies from $6 \cdot 10^{-7}$ to $1 \cdot 10^{-4}$ mol/L.

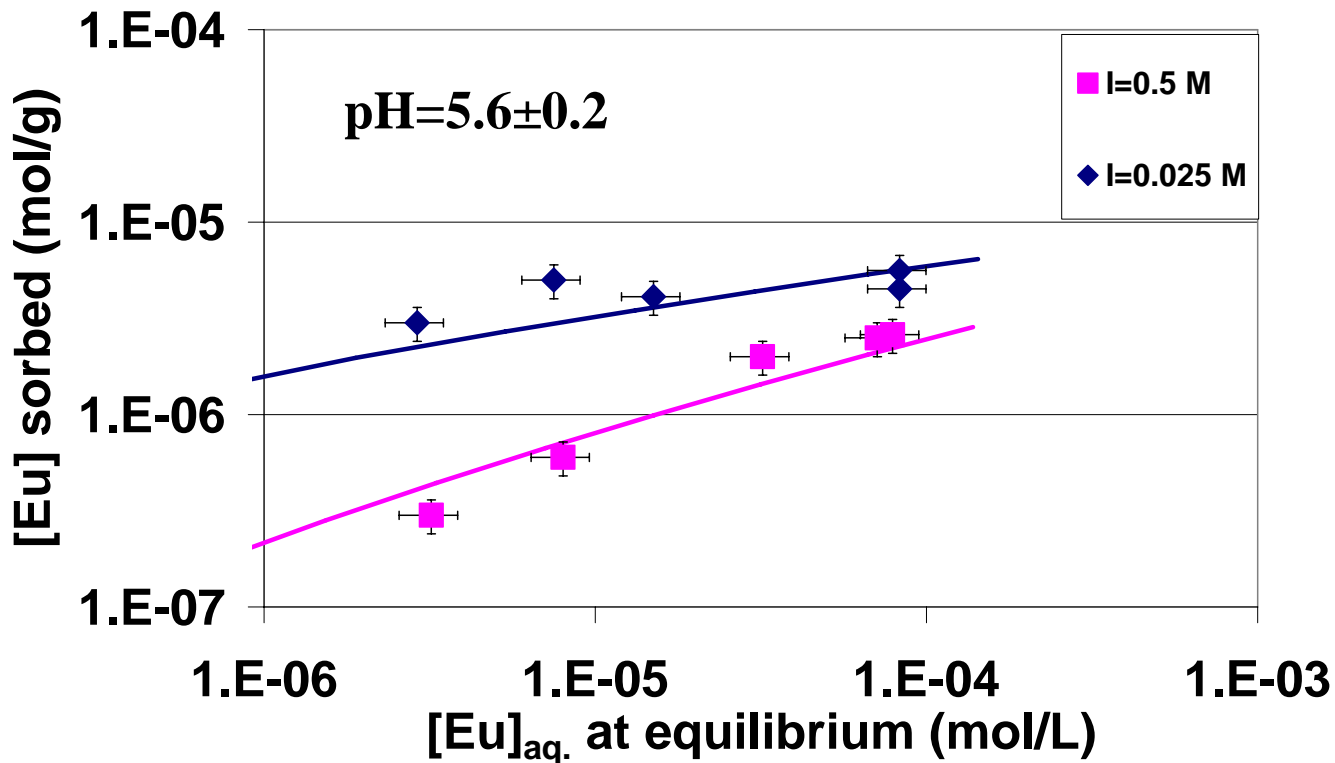


Figure 7: Experimental Eu(III) sorption (symbols) as a function of aqueous europium concentration and ionic strength. Eu sorption conducted with all 14 REE present at identical initial aqueous concentrations. Initial concentrations vary from $6 \cdot 10^{-7}$ to $1 \cdot 10^{-4}$ mol/L. Predictions calculated with the GC model for similar conditions are shown by continuous lines.

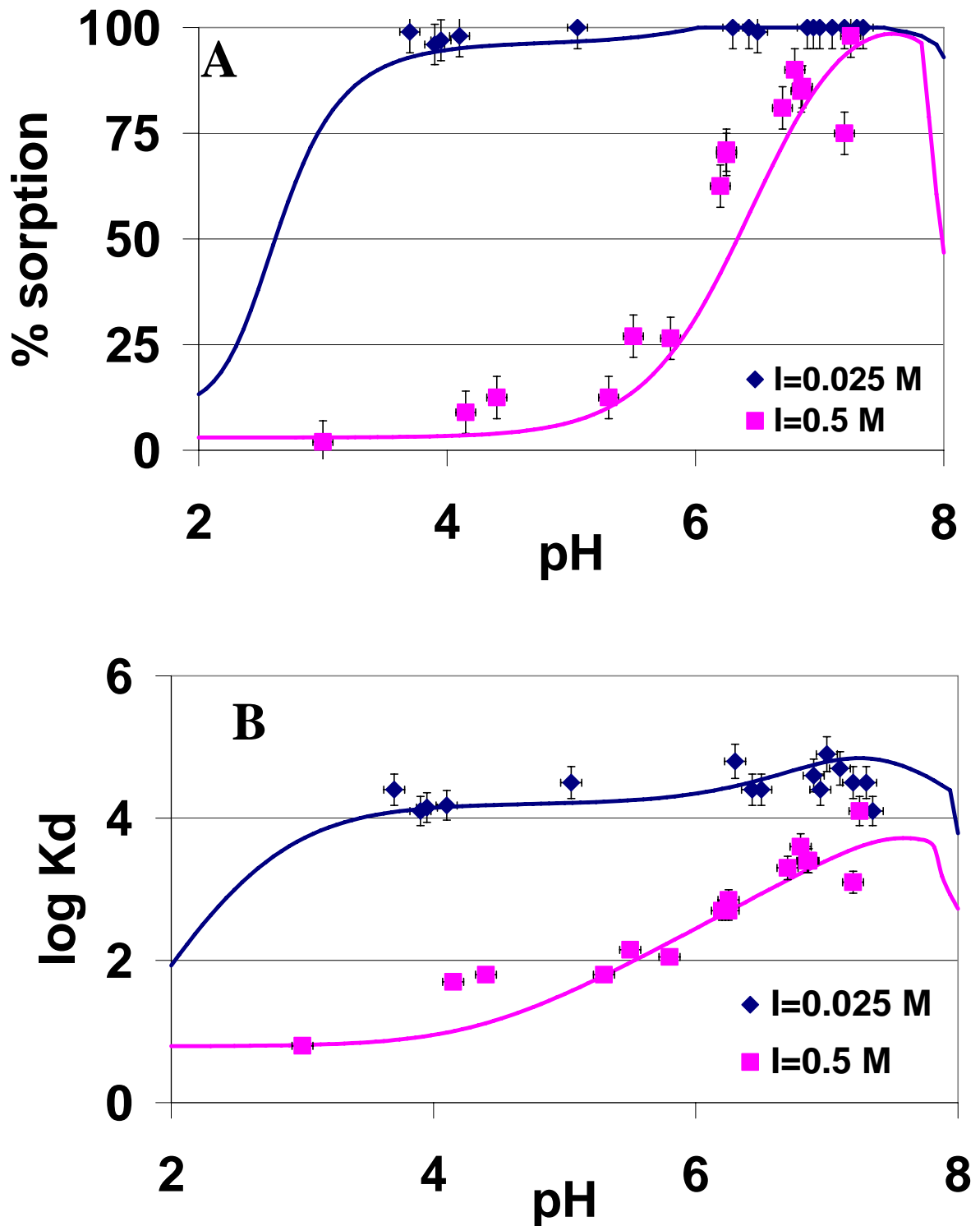


Figure 8 : Experimental Eu(III) sorption data (symbols) for kaolinite (Coppin *et al.*, 2002), as a function of pH and ionic strength. Eu sorption conducted with all 14 REE present at identical initial aqueous concentrations of 130 ppb. Solid lines indicate predictions made with the GC model, without any adjustment. A: fractions sorbed ; B: evolution of distribution coefficients K_d .

Appendix A: Thermodynamic constants used for calculating the aqueous speciation of lanthanides. These constants, used in the CHESS code, are also include in sorption calculations.

Reference	Reaction	-log K 25°C
Tanger and Helgeson (1997)	$H_2O = H^+ + OH^-$	13.995
Helgeson <i>et al.</i> (1981)	$NaCl = Na^+ + Cl^-$	- 0.925
Reported value of Castet <i>et al.</i> (1993)	$NaOH = Na^+ + OH^-$	- 0.455
Ruaya and Seward (1987)	$HCl = H^+ + Cl^-$	- 0.670

Lanthanides	Reaction		
	$REE^{3+} + H_2O = REEOH^+ + H^+$	$REE^{3+} + HCO_3^- = REECO_3^+ + H^+$	$REE^{3+} + 2HCO_3^- = REE(CO_3)_2^- + 2H^+$
	- log K (25°C)	- log K (25°C)	- log K (25°C)
La	8.81	3.60	9.36
Ce	8.34	3.27	8.90
Pr	8.32	3.10	8.58
Nd	8.18	3.05	8.49
Sm	7.84	2.87	8.13
Eu	7.76	2.85	8.03
Gd	7.83	2.94	8.18
Tb	7.64	2.87	7.88
Dy	7.59	2.77	7.75
Ho	7.56	2.78	7.66
Er	7.52	2.72	7.54
Tm	7.39	2.65	7.39
Yb	7.24	2.53	7.36
Lu	7.27	2.58	7.29
Reference	Klungness and Byrne (2000)	Luo and Byrne (2004)	Luo and Byrne (2004)

Lanthanides	Reaction		
	$REE^{3+} + 3H_2O = REE(OH)_{3(s)} + 3H^+$	$REE^{3+} + H_2O + HCO_3^- = REEOHCO_{3(s)} + 2H^+$	$2REE^{3+} + 3HCO_3^- + xH_2O = (REE)_2(CO_3)_3(H_2O)_x(s) + 3H^+$
	- log K (25°C)	- log K (25°C)	- log K (25°C)
La	20.28	-	- 4.31 (x=8)
Ce	19.88	-	- 4.11 (x=8)
Pr	19.58	-	- 3.81 (x=0)
Nd	18.08	2.82	- 3.66 (x=0)
Sm	16.48	-	- 3.51 (x=0)
Eu	15.34	2.52	- 5.87 (x=3)
Gd	15.58	-	- 3.71 (x=0)
Tb	15.68	-	- 3.21 (x=0)
Dy	15.88	-	- 3.01 (x=0)
Ho	15.38	-	- 2.81 (x=0)
Er	14.98	-	- 2.61 (x=0)
Tm	14.98	-	- 2.41 (x=0)
Yb	14.68	-	- 2.31 (x=0)
Lu	14.48	-	- 2.01 (x=0)
Reference	Johnson <i>et al.</i> (1992)	Johnson <i>et al.</i> (1992)	Johnson <i>et al.</i> (1992)